SOYMOD/ OARDC –

A DYNAMIC SIMULATOR OF SOYBEAN GROWTH, DEVELOPMENT, AND SEED YIELD:

I. Theory, Structure, and Validation

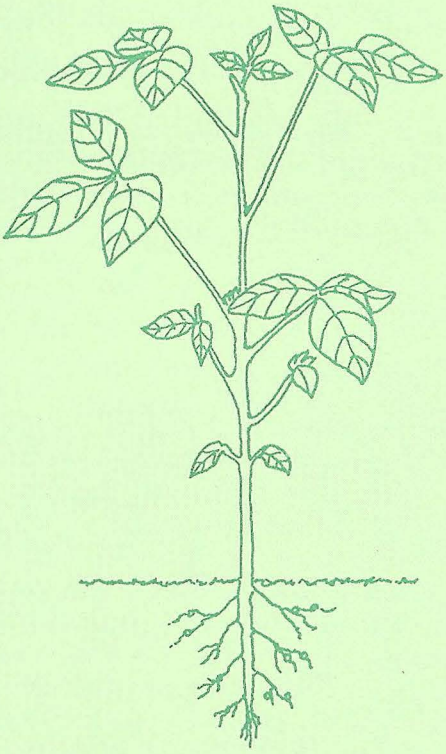

G. E. MEYER

R. B. CURRY

J. G. STREETER

H. J. MEDERSKI

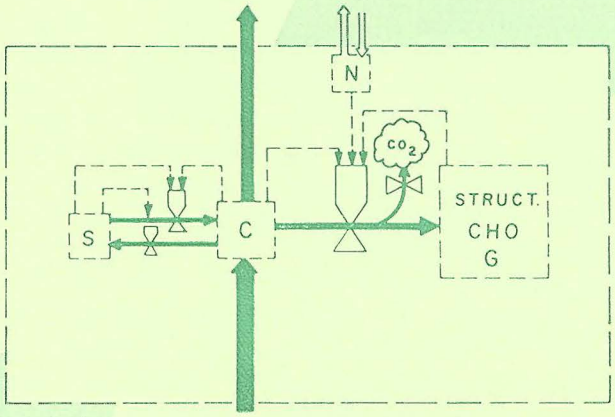

RESEARCH BULLETIN 1113

DECEMBER 1979

OHIO AGRICULTURAL RESEARCH AND DEVELOPMENT CENTER

U. S. 250 and Ohio 83 South

Wooster, Ohio

CONTENTS

*** **** ***

AGDEX 141/07 12-79-2M

SOYMOD / OARDC—A Dynamic Simulator of Soybean Growth, Development, and Seed Yield: I. Theory, Structure, and Validation[1]

G. E. MEYER, R. B. CURRY, J. G. STREETER, and H. J. MEDERSKI[2]

INTRODUCTION

Various quantitative descriptions of physiological processes have been incorporated into a new computer simulator called SOYMOD/OARDC. This simulator succeeds earlier soybean computer models, SOYMOD I (16, 17) and an unpublished intermediate version called SOYMOD II (4) developed at the Ohio Agricultural Research and Development Center.

Previous plant modeling experiences have shown that general patterns of total plant dry matter accumulation can be predicted (11, 14, 22, 39, 41, 55, 73, 74). However, considerable physiological detail is necessary in a soybean simulation model in order to provide levels of information of use to agronomists, plant breeders, or farmers. Several discussions and philosophies in the literature have described principles for conducting plant growth simulation (3, 37, 83). These approaches include both empirical and mechanistic equations. The problems associated with empirical equations are well known. This paper describes a disciplined modeling viewpoint that has been very successful in various fields of engineering and science called the mechanistic approach.

SOYMOD/OARDC is basically a system of dynamic partial differential equations describing the mass and energy balance within the soybean plant. The equations describe the soybean as an open system with import, export, and internal control processes. There is a fundamental underlying hypothesis: SOYMOD is a simulation model of a living solar collector. Solar engineers will recognize the emphasis on solar collection principles, and reliance on collector geometry, with the exception that a biochemical conversion process replaces extensive heat transfer processes.

The reference to a "plant" in this bulletin refers to an "average" plant in a field situation. It is well known that an "average" item does not exist. So, in the case of the soybean, it would not be reasonable to expect to go into a field and find a plant identical to the one described by the model. Mathematical statements used in the simulator were substantiated by a comprehensive review of the soybean physiology literature. Certain process statements, such as photosynthesis and growth, originate from the literature with only minor modifications where they were deemed adequate. Process statements are coupled with appropriate feedback to form the total system. Other process statements concerning fruit abortion, determination of fruit numbers per node, leaf and stem mining, senescence, CHO partitioning, and pod fill processes are new and will be discussed in detail in the next section.

The mechanics of the simulation process also rely on basic principles of plant biochemistry. These principles include product inhibition, enzymatic control, concentration and dilution, mobility of internal nutrients, and buffering. The rate processes are concentration dependent and proceed classically according to simple "rate laws". Some of the soybean rate processes and associated rate constants are temperature sensitive. The new simulator describes in considerable detail the location and intensity of "sources" and "sinks" and how material is partitioned among locations. Source and sink strengths (concentrations) are expressed on a dry matter basis.

Using environmental data over an integration interval as large as 1 hour, SOYMOD/OARDC predicts the total dry matter accumulation for various plant organs: leaf blades, stem and petioles, and fruit at each node on the shoot, and the root system. Total dry matter is subdivided into four basic categories: structural dry matter G, which includes cellulose and other structural polymers; available carbohydrate C, which includes soluble sugars; reserve carbohydrate S; and the nitrogen fraction N, which includes all proteins. The mineral component is not considered. The available carbohydrates may be used as building blocks for new structure or as substrate for assimilation of "new" nitrogen material. The nitrogen fraction is involved in regulatory activity in the production of new dry matter.

A Forrester[3] diagram showing the basic relationship among the dry matter components is given in Figure 1. These components make up the living tissue for the simulated soybean plant. A deficiency of any one of these components has a limiting influence

[1]This research was supported in part by PL 89-106 Grant No 616-15-71 and Grant No. 115-15-116.

[2]Assistant Professor of Agricultural Engineering, University of Nebraska (formerly Post-doctoral Research Associate, OARDC); Professor of Agricultural Engineering, Professor of Agronomy, and Professor of Agronomy, OARDC, respectively.

[3]Based on the symbol conventions of Forrester (30).

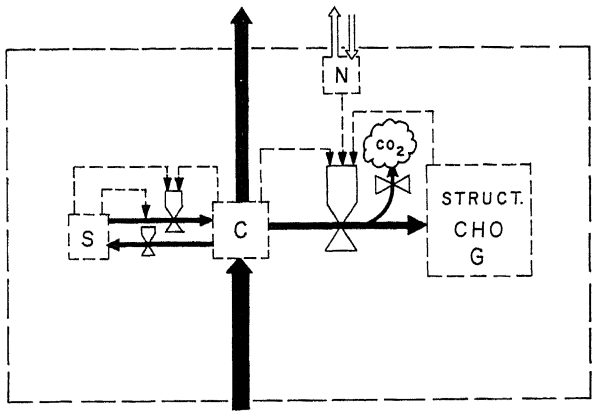

FIG. 1.—Dry matter components used in SOYMOD, where C = available carbohydrate, G = structural carbohydrate, S = reserve carbohydrate expressed as starch, N = protein expressed as plant nitrogen.

over the growth process. During steady-state growth, the relative amounts of each component remain unchanged. This breakdown of components is realistic to work with, since they can be verified experimentally, using standard assay techniques. Water plays an indirect role in the dry matter balance and tissue expansion of the growth process. Water also plays an important role in the regulation of the photosynthetic process, and thus directly affects the production of available carbohydrates.

Node formation, flowering, pod fill initiation, and leaf abscission are considered as discrete events in SOYMOD. These events represent the "current development strategy"[4] during the course of the simulation. During the simulation of vegetative growth, all resources are directed toward maximizing leaf and stem growth. During reproductive growth, resources are directed toward maximizing fruit growth (in terms of dry matter and numbers of pods and seeds). During any instant of time, the mass and energy balance is governed by the current development strategy. During severe plant stress, vegetative or reproductive development can be adversely affected.

SOYMOD/OARDC was programmed in FORTRAN IV and was originally tested on an IBM 370/168 computer, under a MVS operating system, located at The Ohio State University, Columbus. It also has been run on other computers at various locations with only minor changes in the code, including General Automation 18/30, Prime 400, Hewlett Packard 3000, and an IBM 370 CMS system. The current version is running on the HP 3000 at OARDC.

Figure 2 shows a flow diagram of the simulator using standard flow-charting symbols. On the left of the figure is the mainline program logic, while on the right are the subroutines and their location in the calling sequence. Appendix B gives more information concerning each subroutine.

This bulletin describes the details of the major sections of SOYMOD. The description is presented both in terms of the physiological base and the program procedure. It is not intended to serve as a user's manual.

STRUCTURE OF THE MODEL

Appendix A summarizes the differential equations used. The process terms included in these equations are photosynthesis, photorespiration, growth and maintenance respiration, translocation, carbohydrate partitioning, transpiration, nitrogen metabolism and partitioning, and leaf senescence. As mentioned previously, node formation, flowering, podfill initiation, and cotyledon, unifoliate, and trifoliate leaf blade and petiole abscission are considered as discrete events. This section discusses individual process equations associated with the leaves, stem, fruit, and roots, and how each process is modeled.

Photosynthesis

The equation describing photosynthesis at each leaf node (i) was first given by Lommen *et al.* (54) and is represented by subroutine PHOTO.

$$P_S(i) = \frac{[C_A + K + S_1 (P_C(i)-R) - RS_2] - \{[C_A + K + S_1 (P_C(i)-R) - RS_2]^2 - 4S_1 [C_A - RS_2) (P_C(i)-R) - RK]\}^{0.5}}{2S_1} \quad (1)$$

where:

$P_S(i)$ = net photosynthesis (CO_2 flux through stomata) nmole cm^{-2} sec^{-1}

C_A = CO_2 concentration in the free air nmole cm^{-3}

K = a constant equal to c_c (CO_2 concentration in chloroplasts) at which $P_S(i) = P_C(i)/2$ nmole cm^{-3}

$P_C(i)$ = gross photosynthesis at saturating c_c for given absorbed insolation and temperature nmole cm^{-2} sec^{-1}

R = respiration nmole cm^{-2} sec^{-1}

[4]Term coined by Lockhart (53) to describe the genetically controlled temporal and spatial allocations of the resources available to the plant for various functions, such as coping with environmental stress, expansion, and multiplication, but not necessarily in an optimum fashion.

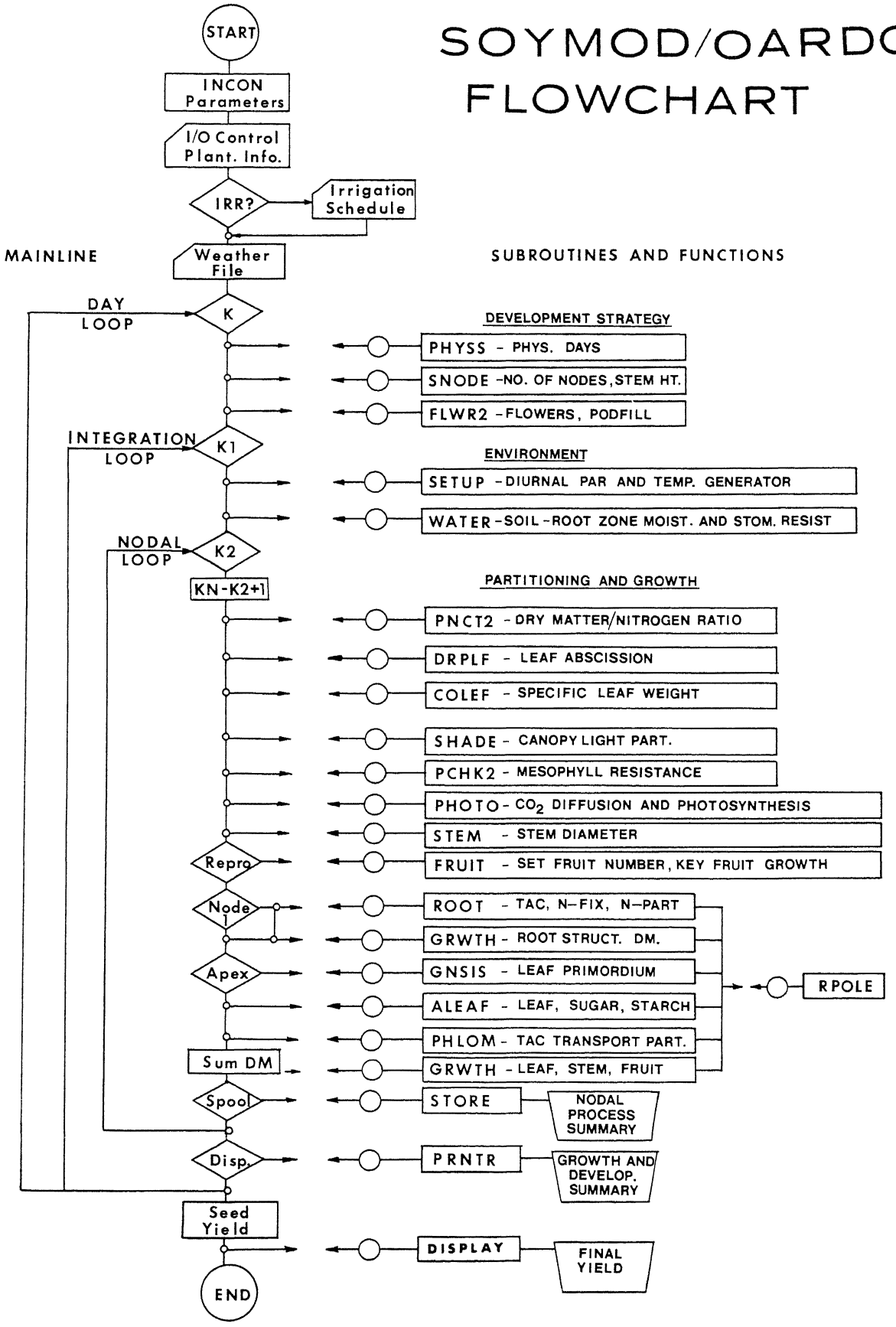

FIG. 2.—Simplified flow diagram of SOYMOD/OARDC, showing flow of logic and program units.

$$S_1 = r_1 + \frac{r_2 (r_3 + r_4)}{r_2 + r_3 + r_4}$$

where: r_1 = stomatal resistance at node i sec cm^{-1}

r_2, r_3, r_4 = mesophyll resistances at node i sec cm^{-1}

and

$$S_2 = \frac{r_2 r_4}{r_2 + r_3 + r_4}$$

The chloroplast CO_2 assimilation rate $P_C(i)$ is calculated according to equation 2 and is offset by a maintenance and photorespiration rate term within the leaf, R. The rate $P_C(i)$ is a function of PAR (Photosynthetically Active Radiation), temperature, and a potential photosynthetic rate $P_M(i)$.

$$P_C(i) = \frac{\phi(T) \cdot E(i) \cdot P_M(i)}{E(i) + K_{PC}} \quad (2)$$

where: E(i) is PAR level at node i

The potential rate of photosynthesis $P_M(i)$ was assumed a function of the leaf nitrogen concentration per unit leaf area at each node by a general relationship developed from data by Buttery and Buzzell (9) and Ojima, *et al.* (65).

$$P_M(i) = C_1 \cdot \phi_{PM}(N) + C_0 \quad (3)$$

where: $C_1 = 30.4$

$C_0 = 0.0$

This equation, as will be seen later, plays an important role in leaf senescence as defined in SOYMOD.

Equation 1 describes the C-3 photosynthetic process rate within a leaf with photorespiration and simplified leaf diffusion resistance network. Stomatal and mesophyll resistances control the flux of CO_2 to and from the sites of photosynthesis. Stomatal resistance, r_1, is controlled jointly by leaf water potential and light intensity. Mesophyll resistances, r_2, r_3, r_4, are controlled by the level of starch buildup in the leaf (63) and will be discussed later. The level of maximum potential photosynthesis (P_M) is governed by the leaf nitrogen concentration at each node (representing important photosynthetic enzymes) and leaf temperature (5, 9, 65, 69). Therefore, photosynthesis is considered at each node (i) on the shoot where leaves exist, according to the light energy available at that nodal layer. The ambient concentration of CO_2 (C_A) is usually assumed constant at 330 ppm, but can be varied during special studies. Figure 3 shows the response of photosynthesis and respiration to temperature used in SOYMOD.

Figure 4 shows the basic photosynthetic response curves to light and aerial CO_2 concentration. Photosynthesis saturates at a PAR level of 1.0 g cal cm^{-2} min^{-1} for these conditions with a CO_2 compensation point at about 0.02 g cal cm^{-2} min^{-1}. Because photosynthesis is assumed to depend on several factors, other response curves will be presented as these factors are discussed later in the text.

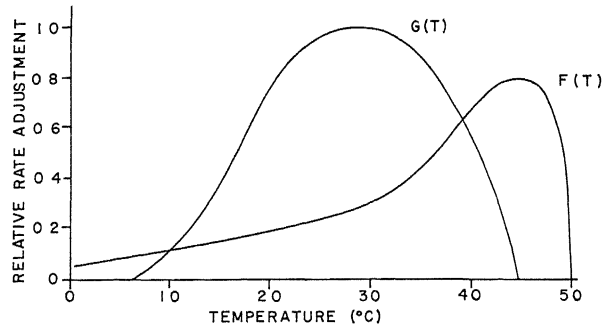

FIG. 3.—Photosynthetic and respiratory temperature response functions. G(T) is the photosynthetic temperature function, F(T) is the dark respiration temperature function.

Light Interception by the Soybean Canopy

An important variable affecting photosynthesis is the spatial variation of light within the soybean canopy. Several simple light partitioning mechanisms have been proposed in the literature, such as the Monteith equation (60) and the Beer's law equation (68). These equations relate empirical attenuation coefficients to the canopy leaf-area-index (LAI). LAI is used in these models as an indicator of leaf overlap. However, there are problems of using the LAI as a continuous overlapping factor because of the leaf and petiole arrangement characteristics of the

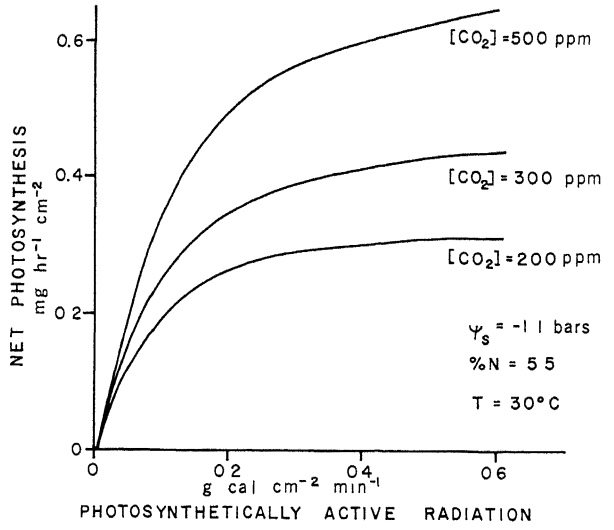

FIG. 4.—Simulated photosynthetic response to ambient CO_2 concentration and photosynthetically active radiation (PAR).

soybean plant. Since light acts as a substrate in the process of leaf area expansion, expansion and petiole orientation occur in the direction of favorable light intensity (19). Thus, for any portion of canopy, *i.e.*, at least two consecutive nodes, the LAI and leaf overlap process over the growing season occur as follows:

$0 \leq LAI < 1$, overlap is not likely to occur (4a)

$1 \leq LAI < 2$, partial overlap has occurred (4b)

$LAI \geq 2$, complete overlap has occurred (4c)

In subroutine SHADE (see Appendix B and Figure 2), the individual petioles and lamina assume positions around the main stem, allowing the most leaf area to be exposed to light with minimum leaf overlap. The maximum possible unshaded leaf area for planophile leaves (*i.e.*, horizontal parallel flat plates) is the maximum area assigned to each plant according to the plant and row spacing. Mature leaves, not subjected to drought stress, are most nearly planophile for soybeans; *i.e.*, representing parallel plates fully exposed to the zenith (6). (In reality, soybean leaves may be slightly heliotropic, tending to follow the sun during daylight. Moreover, this assumption may not be true for water-stressed plants where leaves may assume inclined or vertical orientations.) It was assumed that odd nodal trifoliates shade only odd trifoliates, and even shade only even (alternate phyllotaxy) (see Figure 5). Field observations at OARDC tend to support this assumption.

The ratio of unintercepted light from one even (or odd) node (A_{j+2}) to an even (and odd) node below it (A_j) ranges from 0 to 1 as follows:

$$S_j = (1.0 - ((A_{j+2} + A_j - A_g/2)/A_j), \text{ for } A_{j+2} + A_j \geq A_g/2 \quad (5a)$$

where: A_j = leaf blade area at node j, cm^2

A_g = ground area available, cm^2

S_j = overlap factor

or:

$$S_j = 1.0, \text{ for } A_{j+2} + A_j < A_g/2 \quad (5b)$$

or:

$$S_j = 0.0, \text{ for } A_{j+2} + A_j \geq A_g \quad (5c)$$

Considering Figure 5 and assuming the reflection coefficient, r = 0, the proportion of light available to the next node j-2 is:

$$f_{j-2} = S_{j-2} + \tau(1-S_{j-2}) \quad (6a)$$

where: τ = transmission coefficient

The proportion of light available to node j-4 is then:

$$f_{j-4} = (S_{j-2} + \tau(1-S_{j-2}))(S_{j-4} + \tau(1-S_{j-4})) \quad (6b)$$

and so forth, until j-n is:

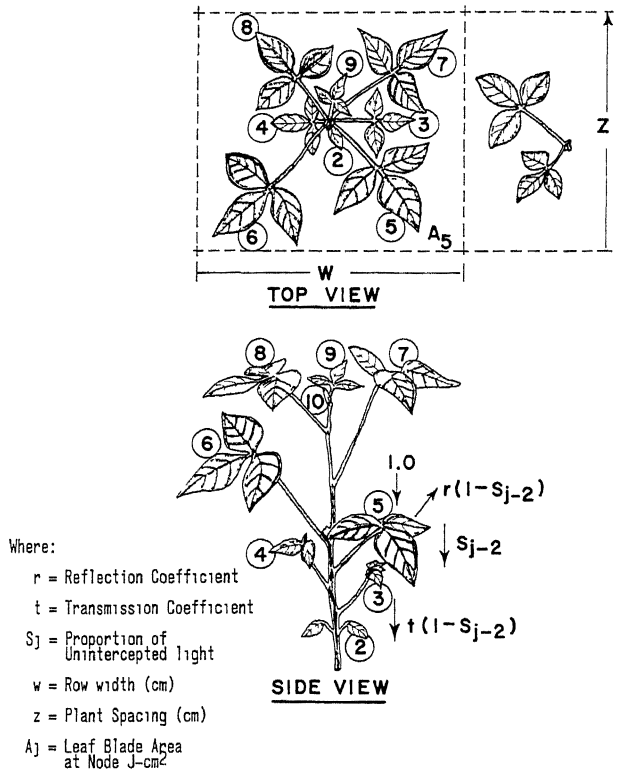

FIG. 5.—Canopy light partitioning and spatial relationships (subroutine SHADE).

$$f_{j-n} = \prod_{j=2}^{j=n} \pi (S_{j-n} + \tau(1-S_{j-n})) \quad (6c)$$

where: j = apical node, odd or even.

Using this procedure, it is possible to describe the canopy effects of soybeans for either uniform planting or row planting distributions. The amount of space given each plant thus governs the amount of self shading.

Considering the assumed planophile nature of the canopy and that most recorded solar radiation data are the normal components of direct and diffuse short wave radiation to a flat, horizontal surface, leaf angle and sun angle are not included in the analysis. It is conceded that additional geometry is needed for inclined or vertical leaves, not presently considered in SOYMOD.

Figure 6 shows a comparison for young plants of subroutine SHADE with Monteith's light partitioning equation (60). (Note that Beer's Law will also produce results similar to Monteith's equation.) The SHADE subroutine does not produce smooth light par-

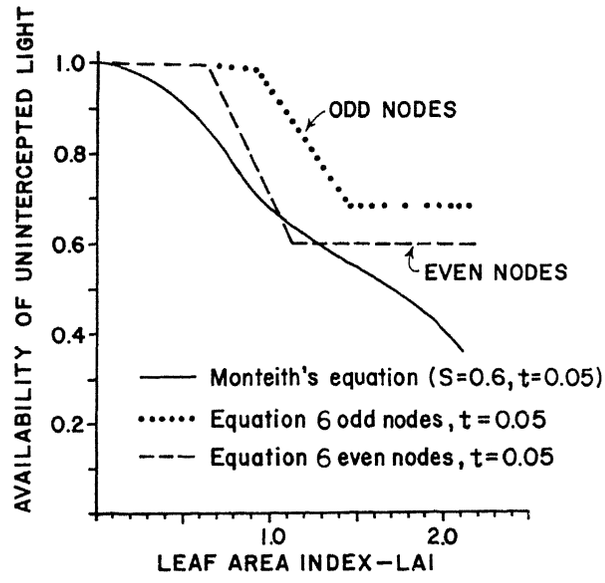

FIG. 6.—Effect of LAI on light interception as simulated by subroutine SHADE or Monteith's equation for a young soybean canopy.

titioning curves, but shows discrete flecking for young soybean plants. Very little self-shading occurs in a young soybean plant of, for example, three or four nodes. Subroutine SHADE accounts for odd-even leaf placement within the canopy, but Beer's Law does not. Subroutine SHADE allows less light to penetrate in older canopies of high leaf area index, but allows more light to penetrate in very young canopies compared to Monteith's or Beer's equation.

Structural Growth

An important term in the mass balance equation for each plant part is the structural growth of the system. Growth is defined as an increase in dry weight, utilizing the carbohydrate generated by photosynthesis and resulting in cellulose. The process of growth requires an adequate supply of available carbohydrate, enzyme material (represented by the N fraction of dry matter), and a supply of chemical energy which can be supplied by either photophosphorylation or oxidative phosphorylation. The authors have chosen to assume that most of this energy is supplied by respiratory processes (growth respiration), and is accounted for in the carbohydrate budget.

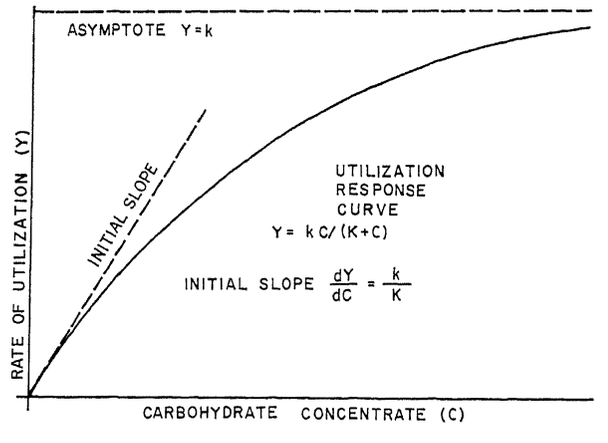

FIG. 7.—Typical growth response function.

While more complex mathematical statements of the enzyme biochemistry of the growth process are possible, a relatively simple but adequate statement describing this process was chosen. The growth process was assumed to proceed according to simplified linear rate laws, summarized by the Michaelis-Menten equation, as suggested by Thornley (82), Hunt and Loomis (44), and others (Figure 7). The concentration of growth "enzyme" used in this expression was assumed to be directly proportional to the amount of nitrogen present in the growing organ. This equation has been applied to many single substrate-enzyme systems (56).

For example, in the case of the fruit, the process of structural growth used in subroutine GRWTH is given as:

$$\frac{1}{G_F(i)}\frac{\partial G_F(i)}{\partial t} = \frac{E_G \cdot K_F \cdot \phi_F(N) \cdot C_P(i)}{K_{MF} \cdot G_F(i) + C_P(i)} \qquad (7)$$

where:

$\frac{1}{G_F(i)}\frac{\partial G_F(i)}{\partial t}$ = the relative growth rate derivative on a structural weight basis, g g^{-1} hr^{-1}

$C_P(i)/G_F(i)$ = concentration of available carbohydrate on a structural dry matter basis, g g^{-1}

$\phi_F(N)$ = function of N content, g g^{-1}

E_G = respiratory efficiency coefficient

K_F, K_{MF} = Michaelis-Menten constants, hr^{-1} and g g^{-1}, respectively

$G_F(i)$ = amount of structural dry matter, g

The parameters K and K_m were estimated for each plant part from limited relative growth rate and sugar content data given by Dunphy and Hanway (23), Howell (43), and data generated during 1976 soybean field experiments. Hanway and Weber (35) observed a maximum soybean growth rate of 0.389 gram per day. The reciprocal Lineweaver and Burk relationship cited by Mahler and Cordes (56) employing a simple linear regression technique was used to find K and K_m from suitable data. Although considerable variation may exist in the magnitude of

these parameters, the average values of K = 0.113 and K_m = 0.08 were found satisfactory during the present stage of simulation work. Interestingly, Hunt and Loomis (44) analyzed tobacco Callus and obtained similar values for these coefficients. However, growth analyses of this type for other crops are usually not available in the literature. These parameters are important and may need to be experimentally determined when not available in the literature.

Respiration

Thornley (83) outlined general concepts for modeling plant respiration which are followed in SOYMOD. These include growth respiration, maintenance respiration, and photorespiration. Each of these processes is related to the available carbohydrate concentration and has an associated conversion efficiency E_G which probably declines with the age of the material (45). Using information provided by Penning de Vries (67), a growth respiration efficiency of 0.75 was initially set for each respiratory site.

Maintenance respiration R which involves the use of carbohydrate for rebuilding enzyme systems and proteins was accounted for in each leaf only. Maintenance respiration was approximated as a rate process related to the leaf dry matter at each node. Thus, the larger the leaf, the more energy that was required for maintenance purposes. Maintenance respiration is also considered to be a function of temperature with a Q_{10} of approximately 2.0.

Photorespiration found in C-3 plants was approximated according to a rate per unit leaf area as a function of light and temperature. The net rate of photosynthesis given by equation 1 was reduced 14% to allow for photorespiration.[5]

Leaf Reserves

The time derivative for the available carbohydrate balance for the leaf (subroutine ALEAF) includes all rate changes due to photosynthesis, photorespiration, maintenance respiration, structural growth, starch accumulation, and TAC (Total Available Carbohydrate) export to the phloem. Some of the carbohydrate produced through photosynthesis is converted to a reserve component which is not available for structural growth, but can be utilized later.

Reserve carbohydrate deposition is modeled as a reversible sub-system temporarily storing about half of the carbohydrate over a given integration interval. This appears to agree with the starch analyses of Warrington, *et al.* (86). The rate of conversion of available carbohydrate to starch is modeled as a second-order process while the return of starch to available carbohydrate is a first-order process.

[5]F. W. T. Penning de Vries, personal communication.

$$Q_L(i) = \frac{G_L(i) \cdot K_{SC} \cdot S_L(i) - K_{CS} \cdot C_L^2(i)}{G_L^2(i)} \quad (8)$$

where:

$Q_L(i)$ = net rate of conversion, g hr^{-1}

$S_L(i)$ = starch concentration, g g^{-1}

$C_L(i)$ = available carbohydrate converted, g g^{-1}

K_{SC}, K_{CS} = rate constants, hr^{-1}

$G_L(i)$ = structural carbohydrate content of leaf, g

The accumulation of leaf starch may affect the level of mesophyll resistance to CO_2 diffusion (63, 80). Therefore, the starch level in the leaf was used to adjust the mesophyll resistance coefficient used in the photosynthetic equation 1 shown in Figure 8 according to Nafziger's equation:

$$r_2, r_3, r_4 = 3.56 - 0.64 \frac{S_L(i)}{A} + 0.53 \left[\frac{S_L(i)}{A}\right]^2 \quad (9)$$

where:

r_2, r_3, r_4 — mesophyll resistances at each node, sec cm^{-1}

$S_L(i)/A$ = starch per unit leaf area, mg cm^{-2}

As starch accumulates within the chloroplasts, the diffusion resistance of CO_2 moving toward the assimilation site within the chloroplast is increased, reducing the rate of CO_2 diffusion and thus the rate of photosynthesis. There are more recent unpublished studies contradicting these results. However, this is not a major feedback mechanism in the model as seen by Figure 8. The authors therefore do not claim proof or disproof of the starch feedback me-

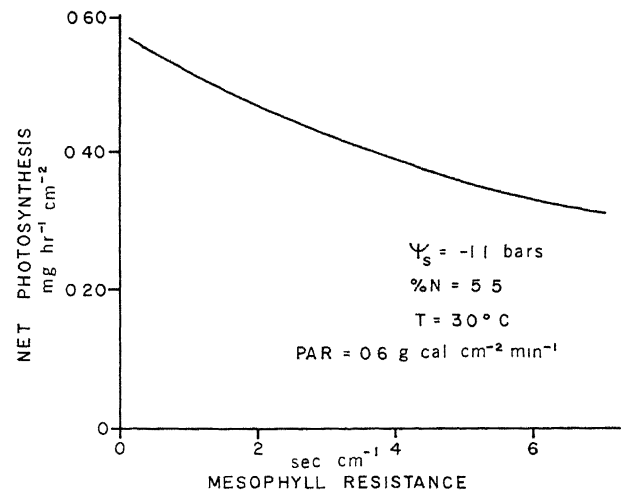

FIG. 8.—Simulated photosynthetic response to mesophyll resistance.

chanism in soybean photosynthesis, but merely include it on the basis of published literature.

Phloem Loading

The process of loading sugar L(i) into the phloem from each leaf node was described as a second order process.

$$L(i) = K_{LP} \cdot \left[\frac{C_L(i)}{G_L(i)}\right]^2 \quad (10)$$

where:

K_{LP} = loading rate constant, hr^{-1}

$C_L(i)/G_L(i)$ = carbohydrate concentration, g g^{-1}

Equation 10 was used for the export of sugar from all leaves except the apical leaf. The apical leaf exported sugar directly to the newly developing leaf, using a first-order, rate process.

$$L(i) = K_{LP}\ C_L(j)/G_L(i) \quad (11)$$

where:

j = apical node.

The leaf area at the various nodes was computed from leaf dry matter using a function shown by Figure 9. This section completes the discussion of the terms of the leaf carbohydrate balance subroutine ALEAF. The authors have concluded that these terms are required to adequately describe the balance. There may be disagreement among the readers as to the actual form of equations of some of these terms. However, the terms selected represent relatively simple approximations until research provides better ones.

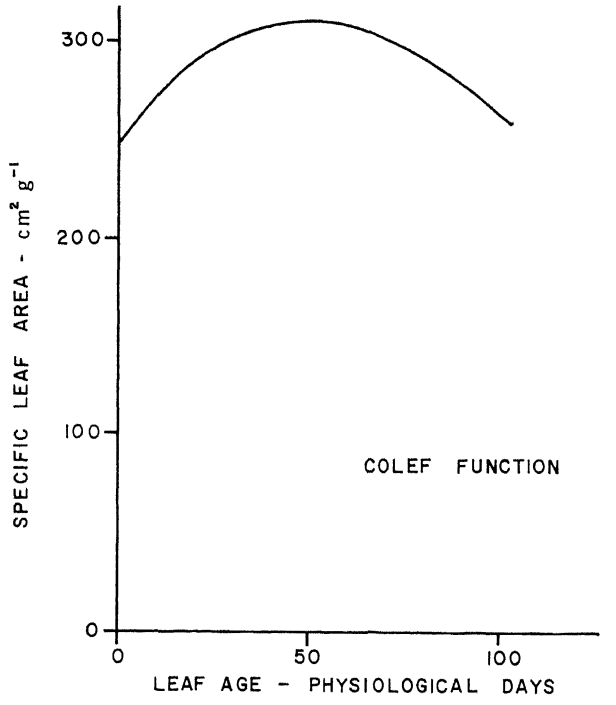

FIG. 9.—Relationship between specific leaf area and leaf age based on 1974 Wooster field data. Used as COLEF function in SOYMOD/OARDC.

Phloem Transport

This section covers some of the terms for the time derivative for the available carbohydrate balance of the stem and petioles. Although various theories have been proposed for phloem transport, an appealing process to many plant scientists involves mass flow driven by a pressure gradient within the sieve tubes (64). This process can be simply derived from the Poiseuille and Van Hoft equations. One of the earliest proponents of mass flow was Munch (61). More detailed versions (which are beyond the current scope of this simulator) have been proposed recently by Christy and Ferrier (12, 27).

The dynamic energy available to drive a sucrose solution through a single sieve tube can be estimated from the concentration of solute within the tube, influx of water from supporting tissue, and influence of gravity. In SOYMOD, water potential is assumed to have no limiting effect on the translocation process. Therefore, a transport term was composed of a velocity and a concentration gradient. The instantaneous sugar transport rate for a section of stem was given as:

$$F = \frac{\beta \cdot n(i) \cdot T \cdot A^2_S \cdot C_P(i)}{8\eta \cdot G^2_S(i)} \cdot \frac{\partial C_P(i)}{\partial y} \quad (12)$$

where:

F = rate of sugar transport, g sec^{-1}

β = is the universal gas constant, 8.314 x 10^7 dyne cm $mole^{-1}$ $°K^{-1}$

A_S = sieve tube cross-section area, cm^2

T = temperature, °K

n(i) = effective number of sieve tubes

η = phloem sap viscosity as a function of sap concentration and temperature, cp

C_P/G_S = sugar concentration, g g^{-1}

$\frac{\partial C_P(i)}{\partial y}$ = sugar gradient between successive nodes, g cm^{-1}

G_S = stem structural carbohydrate, g

The sugar gradient $\partial C_P/\partial y$ was approximated as a backward difference between nodal sections as $(C_P(i+1) - C_P(i)/\Delta y(i))$.

This analysis is based on a single tube element cross-section which is extended to the entire stem cross-section. The number of sieve tube elements was computed according to average sieve tube di-

ameter given by Fisher (28), Housley and Fisher (42), and the stem diameter computed using subroutine STEM. A single chain of sieve tubes was assumed around the outer perimeter of the stem cross-section (assuming a cylindrical section) shown by Figure 10. The total number of sieve tubes "n", of diameter "d" is:

$$n(i) = \frac{\pi\ (D_S(i) + d)}{d} \qquad (13)$$

where:

$D_S(i)$ = stem diameter, cm

d = sieve tube diameter assumed constant, cm

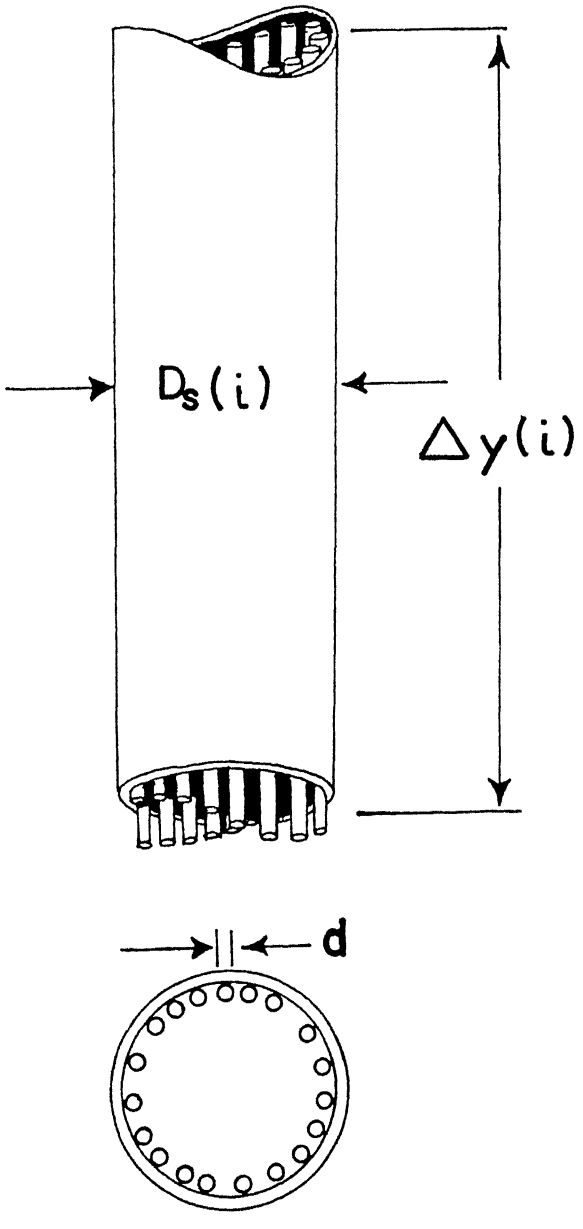

FIG. 10.—Simulated phloem sieve tube and stem geometry of SOYMOD (subroutine STEM).

Assuming a cylindrical internodal stem section, the stem diameter can be computed from the amount of structural dry matter accumulated and the internodal length as:

$$D_S(i) = 2\sqrt{\frac{DM_S(i)}{\Delta y(i) \cdot \rho_s \cdot \pi}} \qquad (14)$$

where:

ρ_s = stem density of 0.50 g cm^{-3}

$DM_S(i)$ = stem dry matter, g

$\Delta y(i)$ = internodal length, cm

The mass flow driving force as a function of sucrose concentration is shown for a constant temperature of 25° C and 1800 sieve tubes in Figure 11. The maximum driving potential for mass flow rate occurred at a concentration of 24%, weight basis. Above 24% concentration, the effect of viscosity tends to reduce the flow rate. Below 24%, the force weakens as the solution becomes more dilute. Other factors such as the hydraulic conductivity of the sieve plate pores or increased flow resistance due to plugging by callose are not considered. In this version, the total transport through the stem can be limited by the amount of sugar available, temperature, the sugar gradient along the stem, and the number of sieve tubes available. A similar analysis was recently presented by Lang (48, 49).

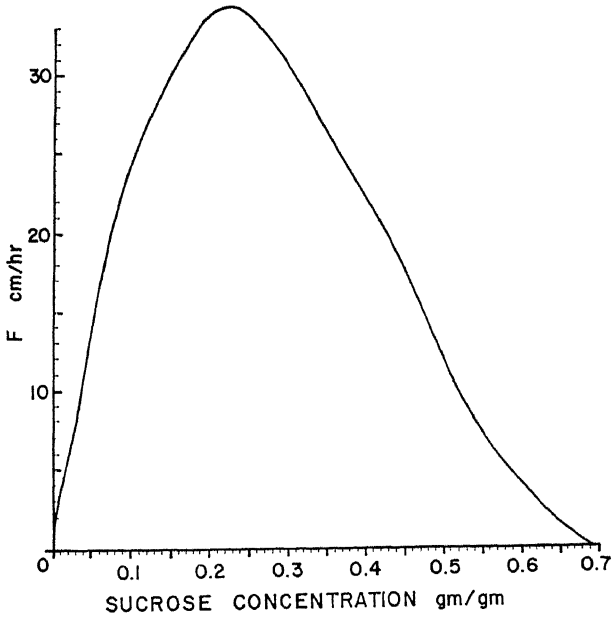

FIG. 11.—Simulated phloem driving force response to sucrose concentration.

Phloem Unloading

The phloem system supplies sugar for the shoot, root, and nodule system for nitrogen assimilation. To simplify the analysis, the phloem compartment was used as a common supply for both the stem and fruit. Equation 7 was then used to compute the growth of each nodal section of stem and the growth of the fruit attached to that node using the Michaelis-Menten growth function. The source strength was implicitly used to determine the number of fruit retained at each node. This calculation was performed at the advent of podfill at each node. Carbohydrate not used at a given node was transported according to equation A9 (Appendix A) to the next lower node, and so forth. The remainder from the shoot was available to the root system. The complete phloem mass balance is described in subroutine PHLOM.

Senescence

Photosynthate is the most dominant term in the mass balance during vegetative growth. Yet it perplexes physiologists and plant growth modelers as to what physiological events occur within the leaf which cause it to lose photosynthetic capacity with age. The loss of photosynthetic capacity with age has been shown experimentally in soybeans recently (62, 88, 89). The authors have attempted to describe this phenomenon in a systematic way. Basically, the current photosynthetic rate is governed by light intensity, temperature, CO_2 concentration, stomatal and mesophyll resistance (equation 1). By describing the canopy as a system of node layers, the level of photosynthetic capacity can be quantitatively considered at each layer depending on the internal leaf conditions and amount of light available at that layer.

In the dark or under low light, the leaves will continue to grow until their available CHO supply is exhausted or until they have outgrown their allotted nitrogen (dry matter/nitrogen ratio reaches 50). Under higher levels of light, leaves will continue to grow as long as photosynthesis is proceeding and nitrogen is not limiting. The nitrogen limiting condition for leaf growth is considered independent of the nitrogen limiting condition for photosynthesis (see Figure 12). Although leaf growth and expansion may temporarily cease, photosynthesis may provide the additional CHO, either for carbon or for nitrogen supply, whichever is needed, so that the process can be restarted.

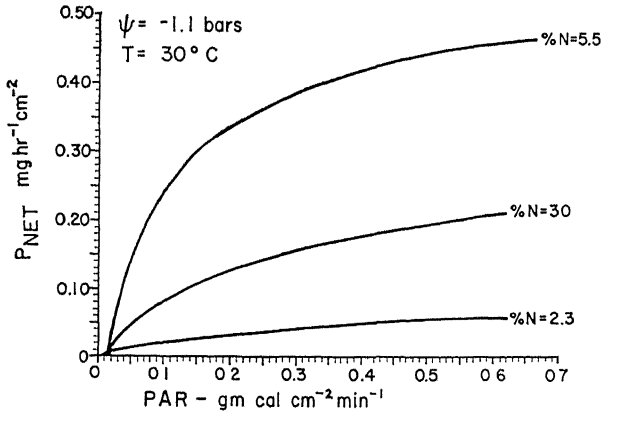

FIG. 12.—Simulated photosynthetic response (PNET) to leaf nitrogen (percent N) and photosynthetically active radiation (PAR).

As the leaf ages, mesophyll resistance may be increased slightly by accumulation of starch (63), or if leaf nitrogen falls sufficiently either from export to the fruit or dilution of the N by continued growth, the photosynthetic capacity is decreased or lost irreversibly. This latter view has been proposed by Sinclair and deWit (71, 72), who argue that plant nitrogen and carbohydrate become deficient so that fruit growth will eventually destroy the vegetative portion of the plant.

There is some evidence in the literature that a hormonal mechanism is involved in the death of the vegetative plant (50, 52). However, the authors have taken the view that a shortage of nutrients in the plant tissue results in senescence, and that the fruit mobilize and remove nitrogen from the vegetative parts. SOYMOD/OARDC includes the concept of competition for nitrogen among all the plant parts. Thus, older leaves must equally share nutrients with younger leaves, and will have lower N concentrations in line with the results of Hanway and Weber (33, 35).

Nitrogen Assimilation

The ratio of nitrogen to dry matter varies between 0.015 and 0.06 on a weight basis during the life of the plants (33, 66, 79). This indicates that the plant has an internal regulating system which can be represented by the function $\phi(N)$, which attempts to maintain a relatively constant dry matter-nitrogen balance. This control subsystem represents a coupling between the carbon and nitrogen balance systems and is a modification of a concept of DM/N control proposed by Duncan.[6]

In order for nitrogen to be available to the shoot tissue, carbohydrate must be first translocated from the leaves to the root nodules. The nitrogen is then fixed by the root nodules, using the carbohydrate as energy, and translocated back to the shoot (subroutine ROOT). This subsystem is modeled as a closed dynamic system, and there is no need to include special demand factors as with other systems (46). The

[6]W. G. Duncan, personal communication.

demand and supply strength is computed by subroutine PNCT2 which explicitly couples the carbon and nitrogen mass balances representing this loop. The term $\phi(N)$ in equation 7 is the function which controls whether growth will proceed in any particular organ. If a low $\phi(N)$ exists in any particular organ, a signal is sent to the nodule system represented as $(1-\phi(N))$ in an attempt to correct the deficiency. The actual physiological mechanism of communication between the shoot and root systems is not presently known.

The nitrogen system of SOYMOD/OARDC has some similarities and differences to the system previously described for SOYMOD I. Basically the nitrogen fixation system is a carbohydrate dependent system (76). The nitrogen input system of SOYMOD is assumed to be the nodule system, although the budget of carbohydrate for a leaf nitrate-reductase system probably would not result in an appreably different energy cost, only in the location of that cost. A significant portion of nitrogen for seed formation can be provided by translocation of N from the leaves, stems, and petioles and pods (33).

The major difference from previous versions of SOYMOD is that the dry matter-nitrogen (DM/N) balance is a consequence of the carbon and nitrogen partitioning systems in a closed-loop form. No standard DM/N ratios are prestored in this model. Growth rates are increased by increased concentrations of internal nitrogen. Growth or photosynthesis (leaves) do not occur below 2% N. The nodule system produces nitrogen according to root carbohydrate supply but ceases when leaf N concentration reaches 6%, stem N concentration reaches 5.5%, or fruit N concentration reaches 8% by weight. In the new system, all plant parts essentially compete for nitrogen from a central source, with each part having a priority dictated by ϕ (N) and a time constant related to use of N to produce structural growth.

$\phi(N)$ is represented by a ramp function for each morphological part. For the leaf blades, stem-petioles, and the root:

$$\phi(N) = 1.0 \text{ for } (DM/N) < 16.7 \quad (15a)$$

$$\phi(N) = 1.50 - 0.03\,(DM/N) \text{ for } 16.7 \leq (DM/N) \leq 50.0 \quad (15b)$$

$$\phi(N) = 0.0 \text{ for } (DM/N) > 50.0 \quad (15c)$$

and for the fruit:

$$\phi(N) = 1.0 \text{ for } DM/N < 14.7 \quad (16a)$$

$$\phi(N) = 22.62 - 1.47\,(DM/N) \text{ for } 14.7 \leq (DM/N) \leq 15.4 \quad (16b)$$

$$\phi(N) = 0.0 \text{ for } DM/N > 15.4 \quad (16c)$$

These assumed functions were derived indirectly from published nitrogen concentrations of plant parts (33). See Figure 13 for the plot of these functions.

In the SOYMOD subroutine ROOT, a constant carbohydrate to nitrogen conversion efficiency independent of soil, plant, or climatic factors was used. Hanson *et al.* (32) reported a low energy cost of 0.79 gram of sugar carbon to produce a gram of soybean seed protein. Penning de Vries (67) reported an energy cost of 1.65 grams of glucose plus NH_3 to synthesize 1.0 gram of protein. This implies that 1.0 gram of glucose will yield 0.11 gram of nitrogen (considering the N content of protein to be 17% by weight (58)). The Penning de Vries conversion factor was used in the model.

Root and Soil Moisture Subsystem

The soil moisture balance (subroutine WATER) consists of rainfall and irrigation as inputs and evapotranspiration (ET) as moisture loss from the soil system. The basic Penman equation modified by Monteith (60a) to include aerodynamic and canopy resistances is used to define the ET process as used in SOYMOD I. Atmospheric diffusion resistance R_a is assumed to be a function of wind velocity $T_a = 8.28/$ wind velocity in m hr^{-1} (20). The canopy diffusion resistance (stomatal control) is computed according to the available light and the leaf water potential (54, 85).

$$r_1 = \frac{E(i) + K_{RL}}{E(i)} \cdot (RSSWP) \quad (17)$$

where:

r_1 = canopy diffusion resistance, sec cm^{-1}

E(i) = PAR at node i, erg cm^{-2} sec^{-1}

K_{RL} = constant – light level which causes ½ max stomatal resistance, erg cm^{-2} sec^{-1}

RSSWP = component of r_1 produced by soil water potential, sec cm^{-1}

The overall minimum resistance was based on a value of 2.5 sec cm^{-1} given by Dornhoff and Shibles (21) and Woodward and Rawson (89).

The computation of soil moisture content and its subsequent effect on plant transpiration takes into account the amount of soil water directly available for root uptake. A moisture balance is calculated for

the soil-root zone. The region containing soil and roots was assumed to be a single compartment or control volume (Figure 14). The volume (V_s) of this region was computed using the current root dry matter and constant average rooting density for the given soil type from the data of Arya *et al.* (2). The shape of the compartment was assumed to be an inverted wedge, with a base area computed from the row and plant spacing. The volume was used to compute the effective root depth which was used in determining the final CHO flux rate from the phloem to the roots. The change in the amount of soil moisture for V_s was:

$$\frac{\partial V}{\partial t} = Ag\,(a_1 R + a_2 I - ET) + E_s \qquad (18)$$

where:

$\partial V/\partial t$ = changes in soil moisture in a given volume of soil, m hr^{-1}

Ag = the surface collection area, m^2

R = rainfall rate, m hr^{-1}

I = irrigation rate, m hr^{-1}

ET = actual evapotranspiration rate, m hr^{-1}

E_s = exchange rate between soil-root system and surrounding soil, m hr^{-1}

a_1, a_2 = infiltration coefficients for rainfall and irrigation, respectively

The volumetric soil water content for the root zone is given as:

$$\theta_v = V/V_s \qquad (19)$$

where:

V = volume of water in the zone, m^3

V_s = volume of soil – root zone, m^3

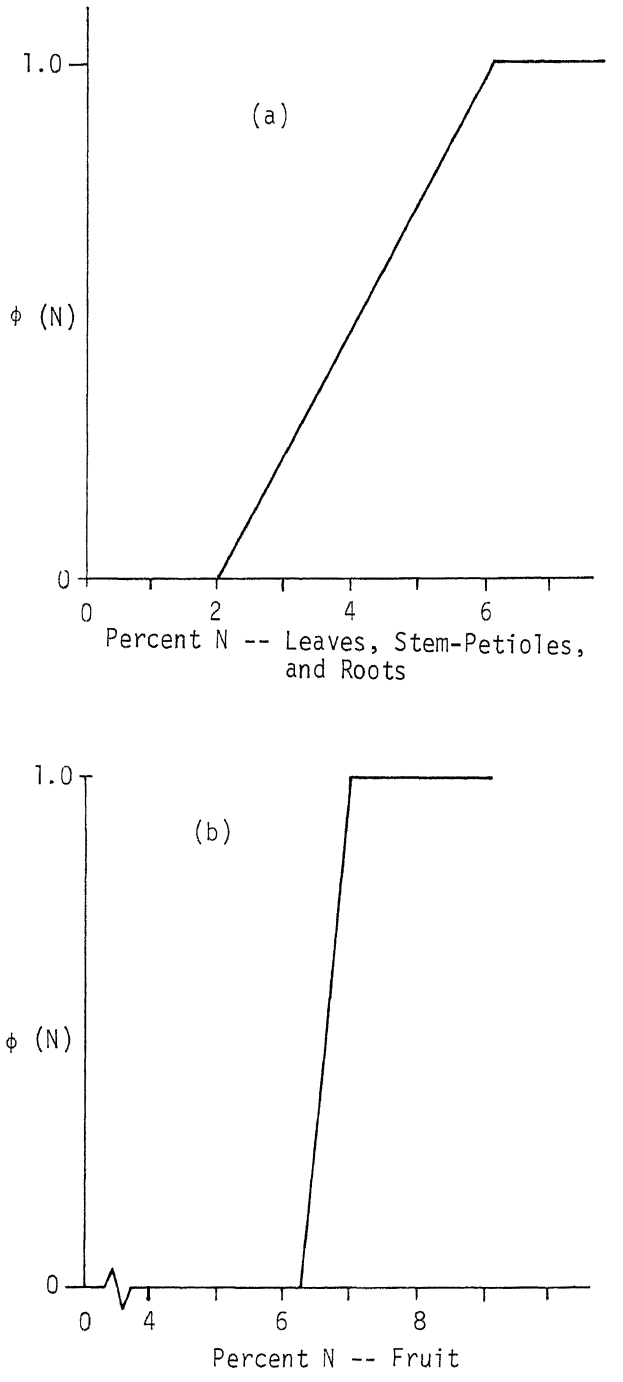

FIG. 13.—Catalytic factors for growth (ϕ/N) as a function of percent nitrogen: (a) leaves, stem-petioles, and roots; and (b) fruit.

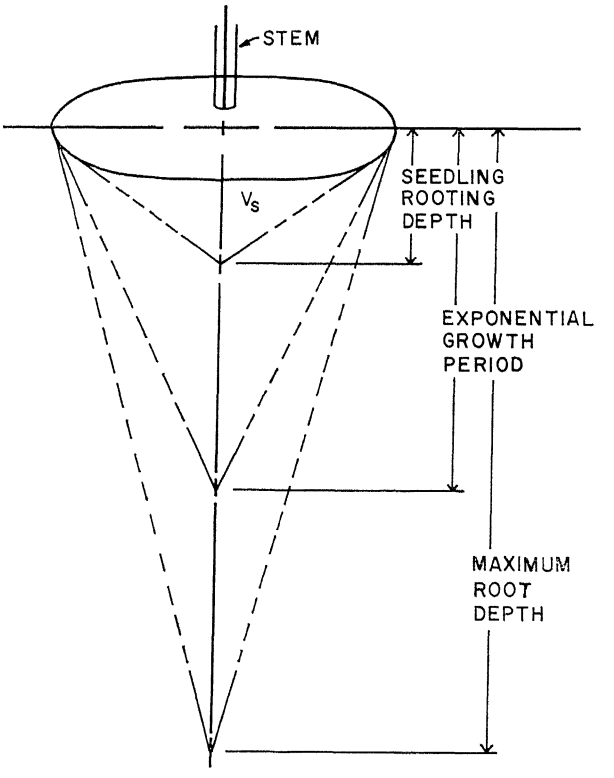

FIG. 14.—Schematic depiction of the dynamic root-soil control volume (V_s) expansion during growing season.

The current soil water content was used to compute the soil water potential. For Wooster silt loam, this equation was developed from data of van Doren (84):

$$\psi_s = 42.6 \exp(-15.8\ \theta_v/\rho_s) \quad (20)$$

where:

ψ_s = soil water potential, bars

ρ_s = bulk density, g cc^{-1}

Assuming a negligible resistance of moisture transport from the soil to the leaf, an equation was developed from data given by Brady *et al.* (7) relating the moisture component of stomatal resistance to soil water potential, RSSWP. Soil water potential ψ_s is assumed to be closely related to leaf water potential.

$$\text{RSSWP} = 2.61 \exp(0.16\ \psi_s) \quad (21)$$

E_s is the term relating moisture exchange between the root system and the surrounding soil.

$$E_s = K \cdot A \cdot \partial\psi/\partial y \quad (22)$$

where:

K = soil moisture permeability, bar hr^{-1}

A = area over which flux occurred, m^2

$\partial\psi/\partial y$ = soil moisture gradient between compartment and surrounding soil, bar m^{-1}

Equation 17 produces a combined resistance due to light and water availability for each existing leaf. In order to combine each resistance into a total canopy resistance, Kirkoff's resistance law was used:

$$1/r^* = \sum_{i=1}^{i=n} (1/r_2\ (i)) \quad (23)$$

where:

r* = canopy resistance used in Monteith's modified Penman equation, sec cm^{-1}

n = total number of nodes with existing leaves

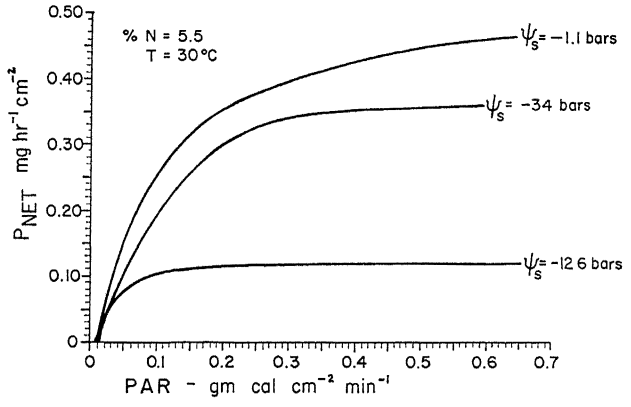

FIG. 15.—Photosynthetic response (PNET) to soil water potential (ψ_s) and photosynthetically active radiation (PAR) for a given leaf N content and temperature.

Figure 15 shows the photosynthetic response to soil water potential.

Using equation 18, the soil moisture was updated every integration interval. This method of handling the root-soil moisture system is a simplified approximation of the real system and further work is needed to delineate a more detailed compartmental system.

As an example of the output of the root and soil subsystem, a comparison of the simulated ET from subroutine WATER and the measured pan evaporation for the 1974 growing season are shown in Figure 16. A summary of literature data would indicate that a well-watered crop in a semi-humid region would have an ET of approximately 0.70 times the pan evaporation.

Discrete Processes

Three basic development processes are described on a discrete basis in SOYMOD. These processes are the timing of new node formation in shoots and the timing of fruit development. Several mathematical approaches to the problem have been suggested. The traditional approach involves the use of an empirical phenological equation (36, 57). Recently Thornley (81) proposed the use of a theoretical morphogen produced by the vegetative tissue and its activity was described by a pair of partial differential equations. When the level of morphogen falls to a certain threshold value, a flower primordium is initiated. The exact identification of this morphogen and its kinetic relationship to the rest of the plant chemistry has yet to be described.

Most development processes involve cell division and differentiation in specific locations and do not replace existing cell structures. The node formation and fruiting phenomena are two key model design problems encountered in plant simulation as opposed to fixed designs used in animal simulation.

The authors have chosen to describe the kinetics of soybean development by the phenological approach, using the equations described below. SOYMOD is flexible and could accommodate any new continuous approaches to development as they become available. These equations essentially involve the identification of new sources and sinks during the growing season based on temperature, daylength, and plant nitrogen content on a discrete event basis.

Development of the Vegetative Shoot: The soybean shoot develops in a systematic way through cell division into leaves, stems and petioles organized in a series of nodes (77). Stage of development descriptions have been given for soybeans (26). However, SOYMOD node numbers differ from Fehr's node system by one to allow for an indexing system in FORTRAN.

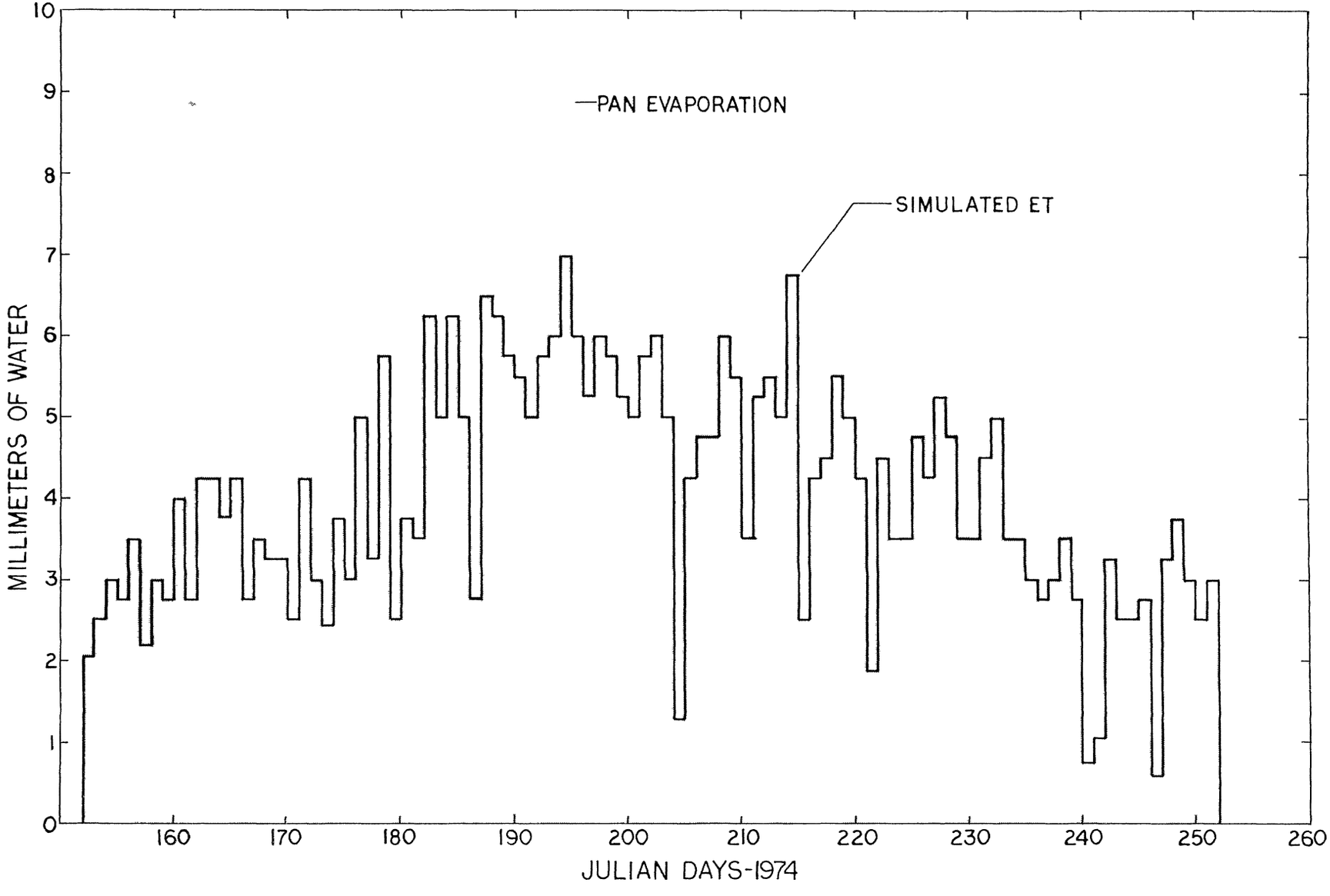

FIG. 16.—Comparison of simulated ET for irrigated soybeans and measured pan evaporation for the 1974 season.

The rate of node formation appears to be closely associated with temperature (40, 69). Node development (subroutine SNODE) is carried on using a physiological day (PHYSD) index system (or normalized heat unit system) where:

$$\text{PHYSD} = \Sigma \text{ Heat Units/HUPDY} \quad (24)$$

Heat units (°C) = daily mean temperature (°C) − 10.

The coefficient HUPDY of 9.0 is the average heat units accumulated per day for the months of June, July, and August based on long term temperature records at Wooster, Ohio. A new node was assumed to occur every 3.7 PHYSD's, based on 1976 field data. When a new node is formed, stem elongation of the new internode is allowed to proceed at a given constant elongation rate to a maximum internodal length over a period of 6 physiological days (supported by growth chamber results carried on during 1976). Node formation and internode elongation were allowed to continue up to a maximum of 18 nodes or when the overall stem dry matter-nitrogen ratio had reached 50 (2.0% N by weight).

Flowering and Fruiting: Another difficult problem confronting soybean modeling efforts is the timing or initiation of flowering and fruiting. It is generally agreed that flowering of short day species is closely associated with daylength and temperature (29, 31, 37, 43). Prior to the reproductive stages, a certain amount of metabolic preparation must occur in order for a plant to flower (competence to flower) (10, 81). Unfortunately, flower initiation is less well-defined than some of the other processes previously mentioned.

The timing of flowering and podfill (subroutine FLWR2) was accomplished using the temperature-daylength iterative regression equation proposed by Major *et al.* (57). While their results show a high correlation for various varieties of soybeans grown in Missouri, this equation has yet to be tested for other locations, emergence dates, or various years of weather data (39). Major's equation takes the form:

$$F(i) = \sum_{j=s_1}^{j=s_2} [a_1 (L_j - a_0) + a_2 (L_j - a_0)^2] \times [b_1 (\bar{T}_j - b_0) + (b_2 (\bar{T}_j - b_0)^2)] \quad (25)$$

where:

- $F(i)$ = flowering index at node 1((if $F(i) = 1.0$, flowering is initiated)
- s_1 = planting date
- s_2 = date of flowering
- L_j = daylength (hr) on the j^{th} day
- $\bar{T}_j$ = average temperature °C on the j^{th} day

For Beeson soybeans, the flowering coefficients given by Major *et al.* (57) are:

s_3 = date of podfill
$a_0 = 8.72$
$a_1 = 0.02435$
$a_2 = 0.002804$
$b_0 = 3.50$
$b_1 = 0.03877$
$b_2 = 0.0$

and

$$P(i) = \sum_{s_2}^{s_3} \hat{a}_1 (L_j - \hat{a}_0) \quad (26)$$

where:

- $P(i)$ = podfill index at node i ($P(i) \geq 1.0$, podfill is initiated), and the podfill coefficients are $\hat{a}_0 = 18.00$; $\hat{a}_1 = 0.01249$

Coefficients for other soybean varieties are stored in a data file in SOYMOD.

When the sum of the series progression involving temperature and daylength equals 1,[7] the flowering or podfill event, depending on the coefficient used, was assumed to occur. A summation was carried out independently at each node above node 3. When flowering was scheduled to occur, 6 flowers were arbitrarily given to that node (a potential of 90 per stem) (38, 78). Major's equation predicts the advent of flowering and podfill from planting date; therefore, the initial values of the accumulators were adjusted to 0.15 to allow computation from the date of emergence. This equation does not take into account internal thresholds which might promote or delay the initiation of flowering.

Some time elapses before mass accumulation begins in the fruit (24). The podfill event generally begins 1 week after the flowering event according to equation 25 for group II varieties. As soon as mass accumulation begins, a decision process is initiated on the fruit number, based on the carbohydrate supply in the phloem and the level of sink strength of the fruit at the given node. This decision in SOYMOD is based on the premise that the individual seed has a growth rate independent of the nutrient status of the parent plant (25). Thus, based on those that could be theoretically supported, the fruit number was adjusted accordingly (subroutine FRUIT). The fruit not supported were considered aborted.

Final seed yield was computed according to the following equation, assuming 28% of the fruit dry matter is pod and that there are three seeds per pod:

[7] The convergence limit of the series is not 1.

$$YD = C \cdot n_P \cdot n_S \cdot S_d \quad (27)$$

where:

YD = dry matter yield, kg ha^{-1}

n_P = number of plants per m^2

n_s = number of seeds per plant

S_d = dry matter weight per seed, g

c = conversion constant = 10 to convert g m^{-2} to kg ha^{-1}

Leaf Abscission: Leaf abscission (subroutine DRPLF) is handled differently and with more detail in SOYMOD/OARDC than in SOYMOD I (17). Leaf abscission was assumed to occur whenever the individual leaf dry matter-nitrogen ratio was greater than 50 (severe individual leaf nitrogen stress) and leaf sugar concentration (not starch) dropped to 0.1% or less. Thus, leaves could be lost anytime during the growing season if the conditions at that node were met. A general leaf abscission process was initiated if the overall leaf dry matter-nitrogen ratio reached 82 (general leaf nitrogen stress). This generally occurred near the end of the growing season after substantial fruit growth. Cotyledons were allowed to abscise when their TAC concentration reached 0.1%, without the nitrogen restriction. Unifoliate abscission was handled in the same way as the trifoliate abscission described above. It was found that this approach resulted in simulated leaf abscission toward the end of the growing season in line with field results.

OPERATION OF THE SIMULATOR

SOYMOD/OARDC is a modular-structured-simulator system written in standard FORTRAN IV for execution on modern segmenting, virtual memory systems, either in the batch or interactive mode. The simulator consists of a mainline program and 21 subroutines of which 18 represent various physiological processes, 1 performs integration, and 2 perform output and spooling functions. The individual names and specific purposes of each subroutine are given in Appendix B. The mainline program acts as an executive system queueing and coordinating the various subroutines in Figure 2.

The system of partial differential equations with the components described was solved using the real-pole numerical explicit technique. This method is available in simulation languages such as CSMP III and DSL and offers increased stability over other single-step techniques such as Euler or modified Euler and decreased computation time over multistep methods such as Runge-Kutta or predictor-corrector. The method is especially valuable in solving "stiff" equations such as the phloem equations. The method is described further by Keener and Meyer (47). It essentially involves a linearization process using the first pair of terms of a Taylor series expansion, separation of terms into a time constant and a forcing function, and using the solution to a first-order ordinary differential equation.

The system of differential growth equations was solved using the real-pole numerical explicit technique (47). This method involves the application of a first-order solution to a linearized equation over a given time interval Δt. Each equation was solved in turn, sequentially. The second order and Michaelis-Menten terms were linearized using the first two terms of a Taylor series expansion.

$$f(C_P) \cong f(C^*_P) + f'(C^*_P) \cdot (C_P - C^*_P) \quad (28)$$

Where C^*_P is the previous value (without nodal notation), about which the expression is expanded. Considering equation A9 and by linear approximation and rearrangement, the result is:

$$\frac{\partial C_P}{\partial t} + Tau \cdot C_P = F_P \quad (29a)$$

where:

$$Tau = \frac{\phi_S(N) K_S}{K_{MS} + C^*_P/G_S} \cdot (1.0 - C^*_P/(G_S K_{MS} + C^*_P)) + \frac{\phi_F(N)\ K_F G_S}{K_{MF} + C^*_P/G_S} \left\{ \frac{1.0}{G_F} - \frac{C^*_P}{G^2_F K_{MF} + G_F C^*_P} \right\} + V_P \quad (29b)$$

and:

$$F_P = V_P C_P(i+1) - \frac{\phi_S(N) \cdot K_S C^{*2}_P}{G_S} \cdot \frac{1}{\left[K_{MS} + \frac{C^*_P}{G_S} \right]^2} - \frac{\phi_F(N) \cdot K_F\ C^{*2}_P\ G_S}{G^2_F} \cdot \frac{1}{(K_{MF} + C^*_P/G_F)^2} + K_{LP}\ G_S\ (C_L/G_L)^2 \quad (29c)$$

where $V_P = \dfrac{\beta \cdot n(i) \cdot T \cdot A^2_S \cdot C^*_P}{8\eta\pi\ G_S \cdot \Delta y(i)}$ (29d)

The solution to equation 29a over the time interval Δt is given by:

$$C_P = \frac{F_P}{Tau} - \left(C^*_P - \frac{F_P}{Tau}\right) e^{-Tau\ \Delta t} \qquad (30)$$

The rest of the mass balance equations were handled in this way and solved sequentially on the digital computer. Using this technique, a typical simulation run over a 120-day growing season using an integration interval of 1 hour took less than 30 seconds central processing unit (CPU) time on an IBM 370/168 MVS system, using the FORTRAN H optimizing compiler.

Input weather data is required on a daily basis and can be selected from a master weather file stored on a direct access device such as disk. The weather data should include date, maximum and minimum temperatures (°F), daily insolation, daily rainfall (inches), wind run (miles), dewpoint (°F), and daylength (hr). The assumption of minimum temperature equal to dewpoint can be used if dewpoint temperatures are not available. Subroutine SETUP converts daily maximum and minimum temperatures and total daily insolation into diurnal temperature and insolation functions, respectively (17). The simulator prompts the user for all other required information at run time as shown in Table 1. This includes output format, row and plant spacing, irrigation dates and corresponding amounts, and initial soil moisture content.

Output is delivered in three formats: 1) a current, environmental input, dry matter, leaf area, fruit

TABLE 1.—Input Data Required for SOYMOD/OARDC.

Plant Data
- Variety coefficients
- Rooting density characteristics for given soil type

Planting Data
- Emergence date, year, month, day
- Row width
- Average plant spacing (stand established)

Climatic Data (daily from emergence to maturity)
- Date, daylength
- Maximum air temperature
- Minimum air temperature
- Dewpoint temperature (or default min. temp)
- Solar radiation
- Rainfall
- Wind run

Soil Data
- Soil type
- Soil water retention curve
- Bulk density
- Hydraulic conductivity
- Initial soil water content

Operation Data
- Choice of output forms: log, partitioning summary and/or short summary
- Print intervals for log and partitioning summary
- Irrigation on or off: irrigation schedule used (or default automatic irrigation)
- Selection of regular run, defoliation, or depodding tests
- Maximum number of days simulated

TABLE 2.—Output Data Generated by SOYMOD/OARDC.

Log (chronology of dry matter accumulation and physiological events)
- Echo of daily weather data
- Total dry matter for leaf blades, stem-petioles, root system and fruit
- Plant height and maximum stem diameter
- Number of fruit
- Flowering and podfill events
- Total leaf area
- Irrigation events
- Leaf abscission events
- Seed yield

Partitioning Summary
- Summary by nodes of dry matter, protein content, soluble sugar content, starch, and fiber for each plant part
- Process rates by nodes: net photosynthesis, respiration, phloem loading, translocation, storage, and growth rates for each part
- Leaf area at each node
- Number of fruits at each node

Short Summary
- Location, date, variety, soil type, and planting configuration
- Total rainfall from emergence to maturity
- Total irrigated water from emergence to maturity
- Total solar radiation and heat units (physiol. days) from emergence to maturity
- Physiological events: flowering, podfill, senescence, and maturity dates
- Crop summary: number of nodes attained
  - Maximum plant dry matter
  - Total evapotranspiration from emergence to maturity
  - Grams per 100 seed
  - Seed yield
  - Total fruit dry matter per plant

numbers summary selectable every day, every 5 days, every 10 days, or final summary only (subroutine PRNTR); 2) a partitioning summary showing process rates and dry matter including soluble sugars, starch, structural dry matter, and protein, leaf area, and number of fruits for each node (subroutine STORE); 3) a final summary giving key phenological events, weather for growing season, and final seed yield and plant dry matter (subroutine DSPLAY).

The user has considerable flexibility in choosing forms of output as shown by sample output in Appendix C. The standard information in each output format is shown in Table 2. Additional information concerning the rate of photosynthesis, storage, and other processes can be also tabulated for each nodal location on the shoot. These assist the user in determining if the simulator is working correctly.

VERIFICATION AND VALIDATION

Various steps were taken to assure SOYMOD/OARDC performance commensurate with field results. The first step was to select soybean field data where sufficient measurements of growth and development and environmental parameters had been made to insure adequate verification and validation. Several performance attributes for comparison of simulated vs. experimental results were selected as follows:

a. Total plant dry weight over time.
b. Total dry weight per plant for the leaf blades, stem and petioles, fruit and root system over time.
c. Dry weight of each plant part per node section over time.
d. Leaf area by node over time.
e. Timing of flowering, podfill, and leaf abscission events.
f. Seed yield at physiological maturity.

In addition to these outward responses, an evaluation was also made of the internal workings of SOYMOD/OARDC:

g. TAC (total available carbohydrates) and nitrogen levels for each plant part per node.
h. Whether or not initiation of new nodes and shoot elongation proceeded in a manner consistent with field studies.
i. Whether or not flowering and podfill initiation intervals were consistent with actual plant behavior.

All of the indicated crop responses can be generated simultaneously using SOYMOD/OARDC. To the authors' knowledge, no other soybean model or multivariate system is currently available which can do this. Using SOYMOD/OARDC, it can be readily determined whether the simulator is predicting yield correctly by concurrently examining the other predicted responses. The process of verification insures that the simulator mimics the behavior of the plant under one set of conditions. Validation, on the other hand, is an ongoing process. It is also important to determine limitations in the model, and in some cases diagnostics have been built into the model to ascertain limitations.

RESULTS AND DISCUSSION

Extensive verification and validation tests indicated in the previous section have been made on SOYMOD/OARDC. This section reports the results of these simulations and compares them with experimental field data. The years of field tests included are 1974, 1976, and 1977. All simulations were begun on the given date of field plant emergence and were performed over the growing season, usually of 120-day duration, using OARDC weather data. The weather data included daily maximum and minimum air temperatures, daily rainfall, daily wind run, and total daily insolation, incident to a flat, horizontal surface. Daylengths were obtained from tables of sunrise and sunset from Naval Observatory data. The soil parameters included bulk density and water retention curve for Wooster silt loam. For each simulation, the average plant and row spacing, initial soil moisture content, and irrigation schedule (if any) were specified. A sample simulation output is given in Appendix C.

1974 Simulation

In order to verify SOYMOD/OARDC for predicting soybean growth and development over a series of given years, it was necessary to calibrate the simulator and check coefficients for a complete and reliable experimental data set. For this purpose, data on Beeson soybeans grown during 1974 were used. These data included dry weights of plant parts and a history of leaf areas taken at frequent intervals during the season. Beeson soybeans (a group II variety) were planted May 15 in 91.4 cm rows. They emerged May 25 and were subsequently thinned to an average 5.6 cm plant spacing. Irrigation was applied during the season, 3.8 cm 17 days after emergence and 22.9 cm during flowering and podfill, for a total of 26.7 cm. The total rainfall for the 120-day season was 31.0 cm.

During preliminary simulations, an adjustment accounting for approximately 0.15 phenological development units was made on Major's equation to account for differences between planting and emergence dates. Without this adjustment, Major's equations tended to predict the events too late. The growth parameters listed for equation 25 appeared satisfactory. The second-order phloem loading co-

efficient, $K_{LP} = 5.0$, was used. Lower values of K_{LP} tended to restrict overall canopy and root growth. Higher values of K_{LP} increased stem and root growth rates initially, but leaf area expansion was eventually curtailed because of lack of supporting leaf growth. The time constants for nitrogen partitioning (see Appendix A) estimated from Hanway and Weber's data seemed satisfactory. The initial condition dry weights for the parts of the emerging plant were estimated from the 1974 field data and are comparable to seed component data.

Figures 17a, 17b, and 17c show the comparison between the simulated and experimental results over the 1974 growing season. Flowering began on July 10 (47 days after emergence) and continued until August 19 (87 days after emergence). Podfill began at node 3 on July 30 (67 days after emergence) and ended at node 17 on Sept. 2 (101 days after emergence). The cotyledons were lost at 60 days after emergence. The trifoliate at node 7 was lost on August 24 (92 days after emergence). Grand leaf abscission began on Sept. 5 (104 days after emergence) and lasted 5 days. The total accumulated physiological days were 122.7 for the 120-calendar-day period, indicating a slightly warmer season than normal.

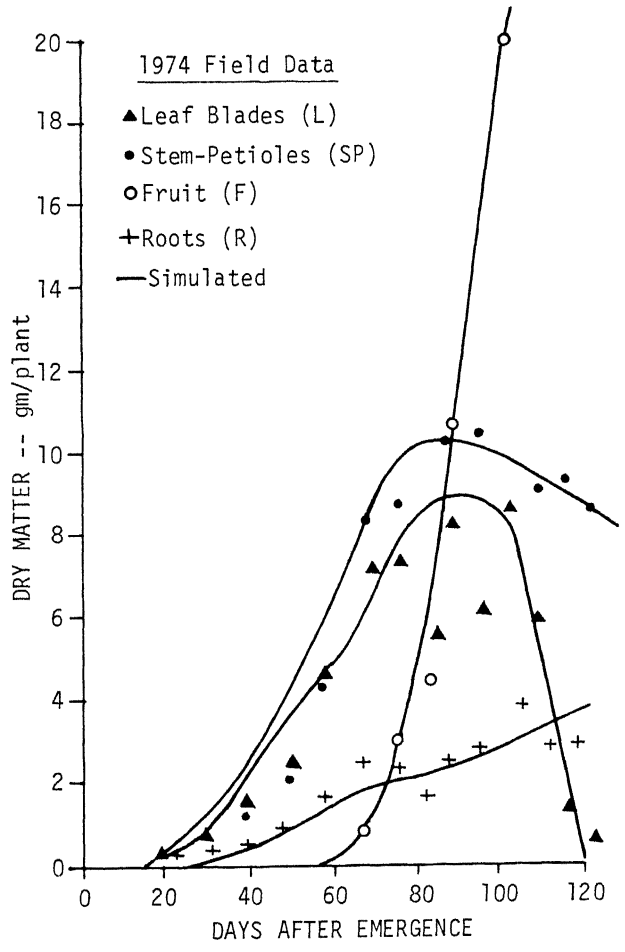

FIG. 17a.—Simulated vs. experimental dry matter for leaf blades, stem, petiole, fruit, and roots for 1974.

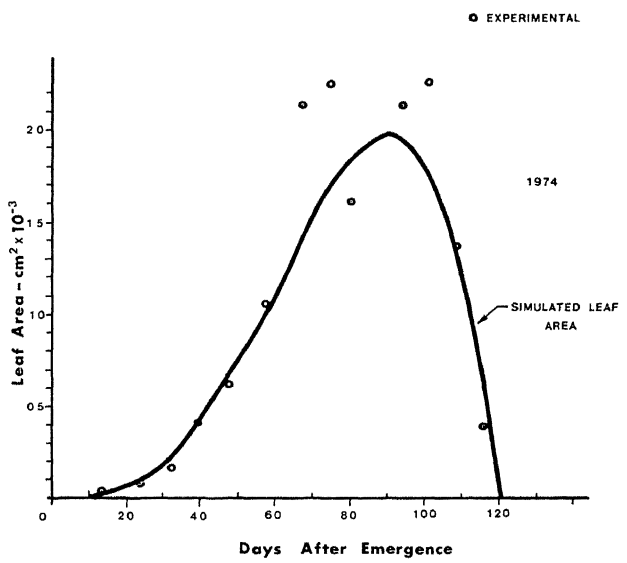

FIG. 17b.—Simulated vs. experimental total leaf area for 1974.

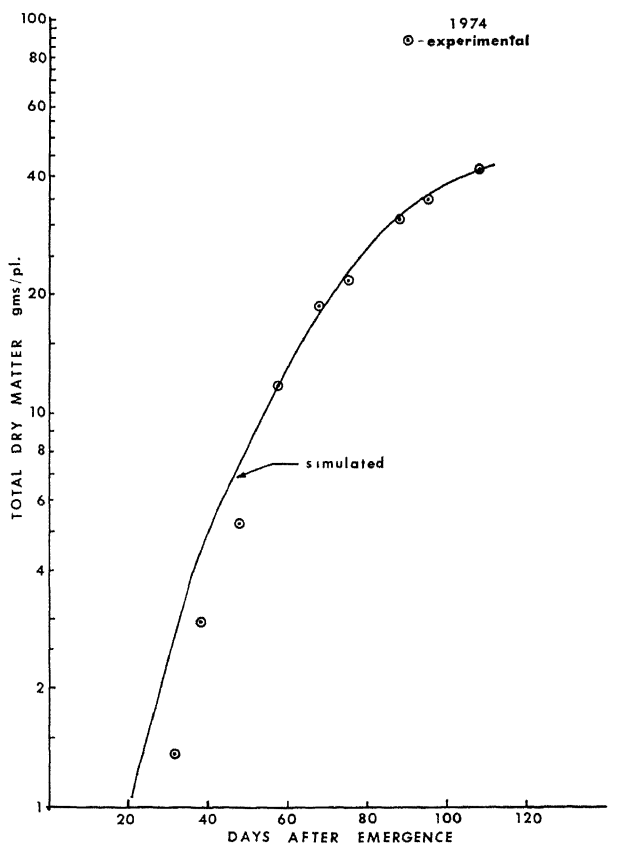

FIG. 17c.—Simulated vs. experimental total dry matter for 1974, semi-log plot.

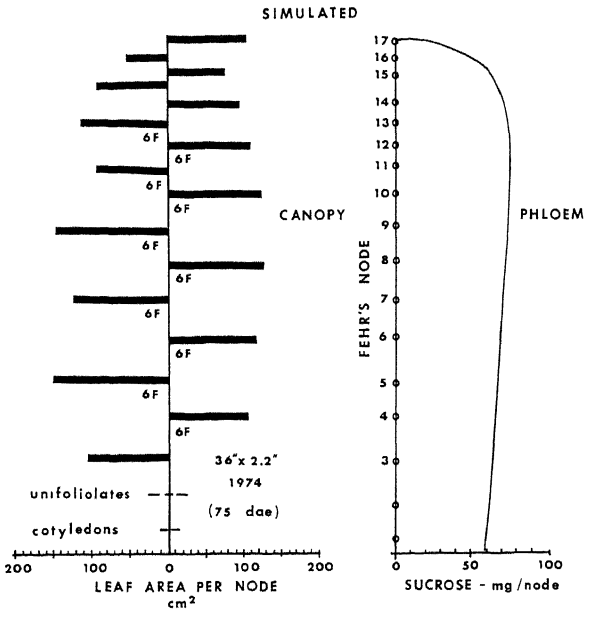

FIG. 18.—Simulated leaf canopy, fruiting, and phloem sucrose content during flowering, 1974, at 75 days after emergence. Plant spacing was 36" x 2.2" (91.4 cm x 5.6 cm).

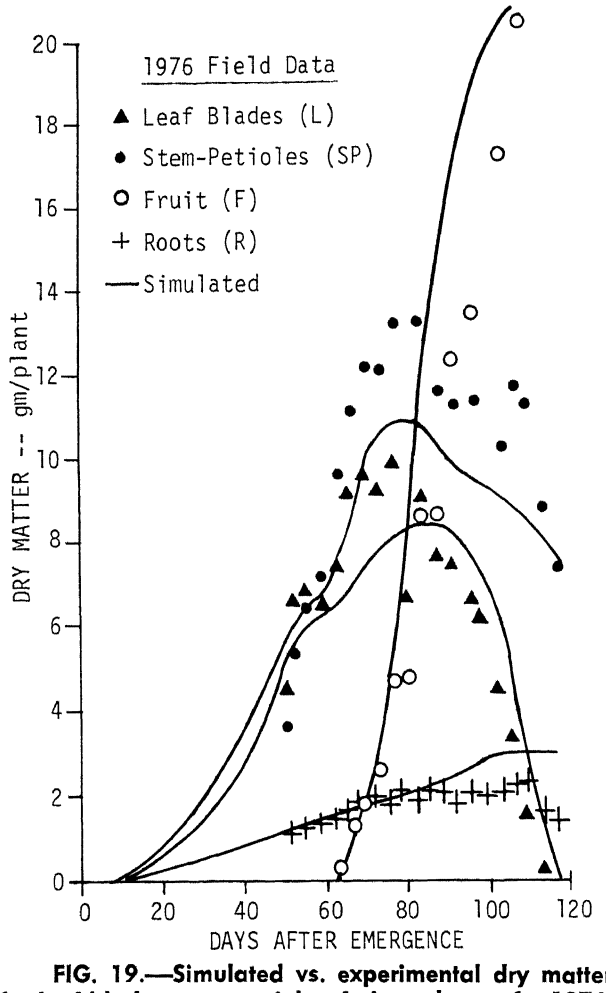

FIG. 19.—Simulated vs. experimental dry matter for leaf blades, stem-petioles, fruit, and roots for 1976.

Figure 18 shows the simulated leaf area and fruit load profile of the soybean canopy on August 7 (75 days after emergence). The maximum leaf area appeared near the center of the main stem. Flowering had progressed to node 13. This figure also shows the amount of sugar present in the phloem for each nodal position. The shape of the phloem sugar content curve suggests that sugar was being loaded into the phloem primarily in the upper half of the canopy and much of this sugar was reaching the root system.

1976 Simulation

With SOYMOD/OARDC calibrated to 1974 field results, the results obtained during the summer of 1976 were simulated. The experimental data used were obtained from a Department of Agronomy study involving several treatments of supplemental reflected sunlight to the soybean canopy. Dry matter and fruit numbers for the control treatment were used. The Beeson soybeans were planted in 76.2 cm rows on May 19 and emerged May 26. Irrigation water had been applied during the growing season in order to hold moisture stress at a minimum, but no record of the amount was available. The automatic irrigation feature of SOYMOD/OARDC was used to hold soil moisture near field capacity for the growing season. The simulated amount of water applied was 11.4 cm.

Figure 19 shows that the calibrated model was capable of predicting the dry matter of the 1976 controls in an acceptable manner. Podfill began July 28 (64 days after emergence) in line with the field results. Table 3 compares the simulated fruit number per plant with the actual data. The fruit numbers were close to actual numbers and appeared to always fall within the standard error of the mean of six replicates of three or four plants each.

The simulated canopy profile for August 20, 1976, (87 days after emergence) is given by Figure 20. The canopy profile for 1976 was conspicuously

TABLE 3.—Simulated and Actual Fruit Numbers per Plant, Summer 1976.*

Date (Days After Emergence)		Actual No. ± S. E.	Simulated No.
8/5	(71)	56.0 ± 7.3	58
8/19	(85)	61.5 ± 6.1	65
9/2	(99)	44.8 ± 1.9	42
9/17	(114)	36.8 ± 2.5	39†

*Beeson soybeans grown in a test plot at Wooster, Ohio. Emerged May 27, 1976. Grown in 76.2 cm (30.0 in) rows, thinned to an average 5.1 cm (2.0 in) plant spacing, and irrigated.

†Final number.

different from the 1974 profile (Fig. 18). Field observations tend to reveal that canopy profiles are closely related to stand density. A more open canopy (19 plants per m^2) like the one of 1974 allows more penetration of light to the leaves of the middle nodes. Leaf growth and expansion and setting of more fruit per node is favored in the lower nodes. The higher stand density (25 plants per m^2) in 1976 tended to favor the occurrence of the largest leaves in the upper nodes. It is more difficult for light to penetrate into this canopy.

The simulation of this crop canopy behavior is very important to the understanding of fruit set in soybeans. Very little data are currently available to validate this; however, data like those of Wiersma and Bailey (87) are helpful. Figure 20 also shows that more carbohydrate was being loaded by the leaves near the top of the canopy than those lower in the canopy. No carbohydrate was being delivered to the root system because the vigorously growing fruit essentially depleted the carbohydrate supply in the lower phloem. These simulated results appear to agree in principle with some of the experimental data presented by Stephenson and Wilson (75).

1977 Simulation

During the summer of 1977, a controlled precipitation differential irrigation study on Beeson soybeans was conducted. Soybeans were planted in 76.4 cm rows and thinned to 40 plants per meter. The soybeans emerged on June 6 and were allowed to grow under normal rainfall until July 15 (the advent of flowering), 44 days after emergence, when the treatment rows were covered with 3 mil black polyethylene plastic to divert further rainfall. Three moisture level treatments were established, each with five random replications, separated by uncovered border rows. Treatment A was irrigated to maintain the soil moisture near field capacity, while treatment C was subjected to near wilting point soil moisture conditions. In treatment B, an attempt was made to maintain an intermediate soil moisture stress.

Although considerably more dry matter samples were taken than indicated by Figures 21a and 21b, only those shown have been analyzed to date. These figures show the corresponding simulated results for treatments A and C. The simulations show approximately 18% more total dry matter for the A treatment. The simulated plant seed yield was 2656 kg/ha (48.0 bu/acre) compared to 2009 (36.3) for the experimental plot data for treatment C. For treat-

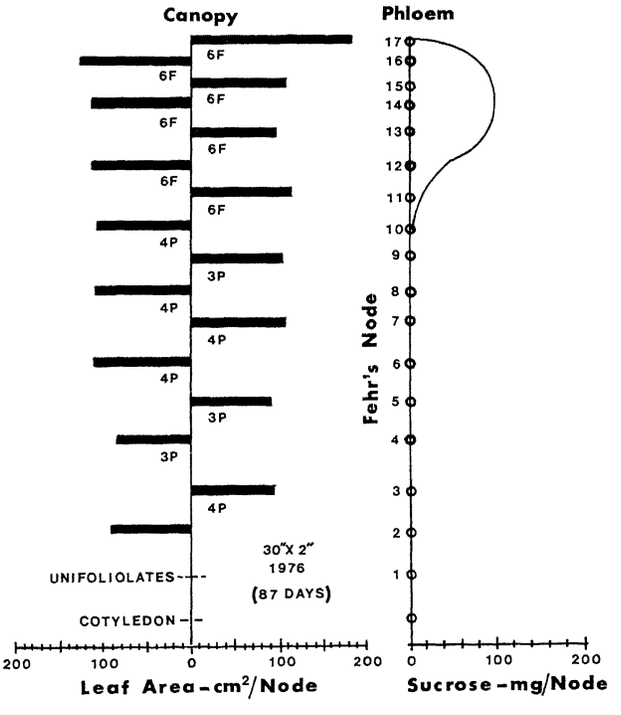

FIG. 20.—Simulated leaf canopy, fruiting, and phloem sucrose content during podfill, 1976, at 87 days after emergence. Plant spacing was 30" x 2" (76.2 cm x 5.1 cm).

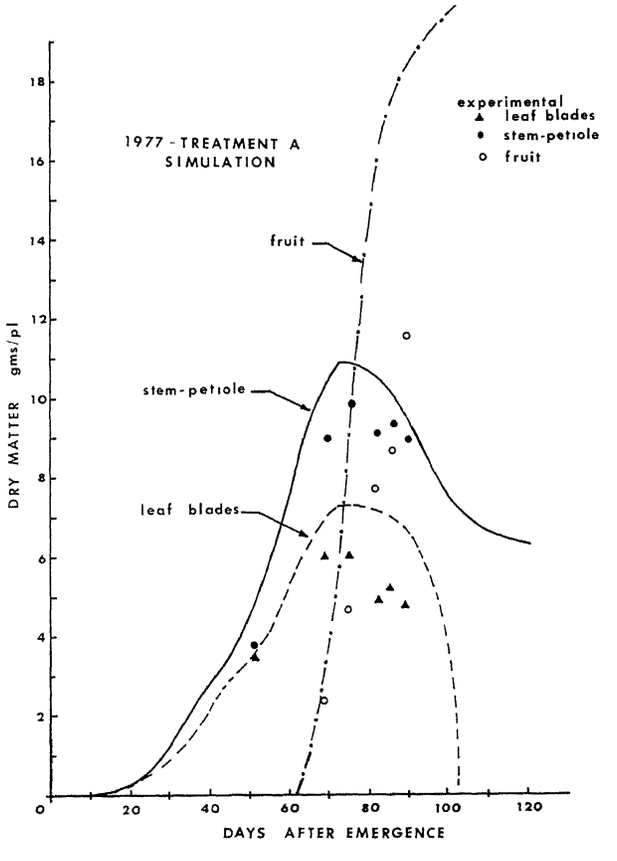

FIG. 21a.—Simulated vs. experimental dry matter for leaf blades, stem-petioles, and fruit for Treatment A (non-moisture-stressed soybeans), 1977.

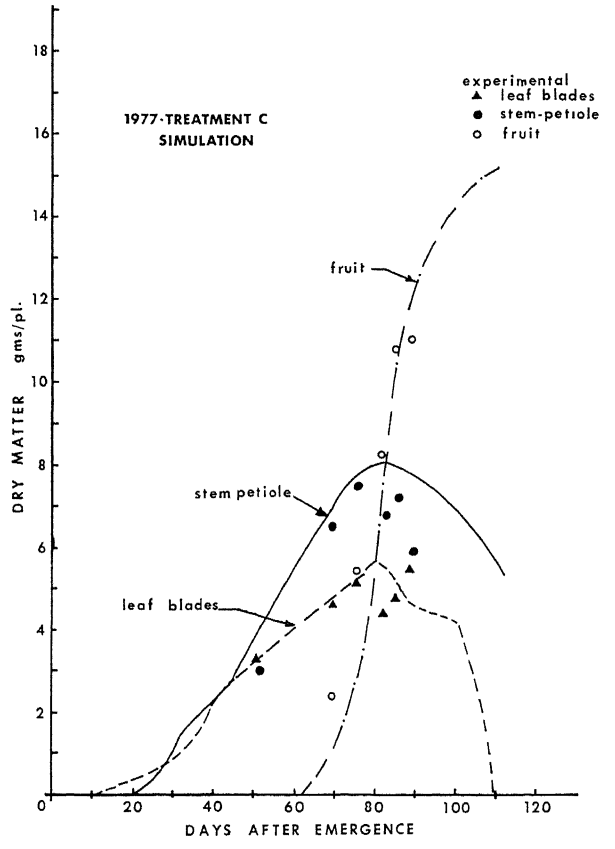

FIG. 21b.—Simulated vs. experimental dry matter for leaf blades, stem-petioles, and fruit for Treatment C (moisture-stressed soybeans), 1977.

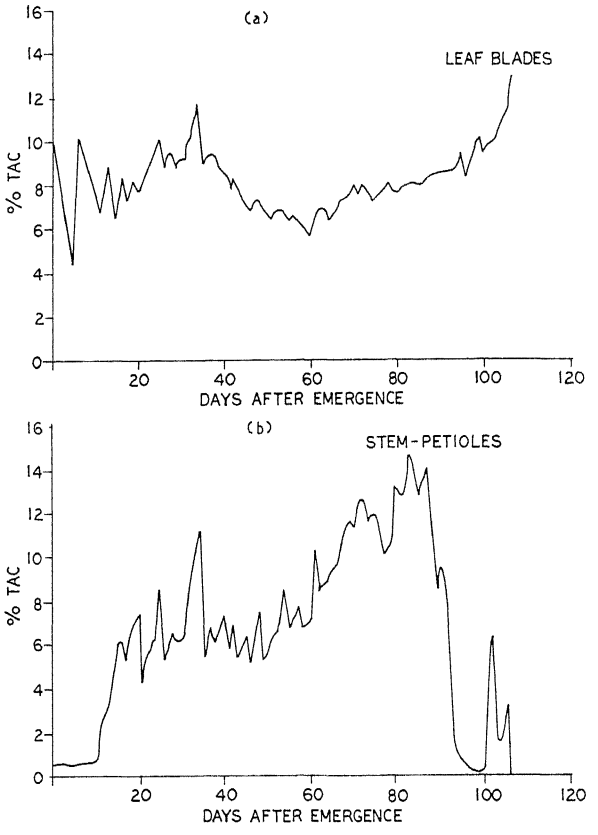

FIGS. 22a and 22b.—Simulated total available carbohydrate (TAC) for successive stages of growth for 1974, (a) leaf blades and (b) stem-petioles.

ment A, the simulated plant seed yield was 3109 kg/ha (56.2 bu/acre) compared to plot yield of 2219 kg/ha (40.1). Thus, treatment C was off by 24.4%, while treatment A was off by 28.6%. The simulated seed yields may have been high for at least two reasons: 1) considerable insect damage occurred in the field but the simulator does not account for this, and 2) the soil moisture subroutines are only first approximations and may not have mimicked the soil moisture stress accurately enough.

Simulated Carbohydrate and Nitrogen Concentrations

Using the growth and storage differential equations shown in Appendix A, total available carbohydrates TAC, which are assumed to comprise both readily available carbohydrate C and starch S, and the plant nitrogen content N are computed on a continuous basis during the growing season. The performance of SOYMOD/OARDC depends on how well these concentrations mimic the real plant behavior. Figures 22a and 22b show TAC concentrations for the leaf blades and stem-petioles simulated for the 1974 growing season. These simulated values compare favorably with data in the literature (8, 23).

The simulated leaf blade concentrations show oscillations on a daily basis, as would be expected from the diurnal input function of photosynthesis. Corresponding pulsations of simulated carbohydrate concentrations are also seen in the stem. Plant growth depends partly on the movement of carbohydrate from the leaves to the nonphotosynthetic parts and partly on plant nitrogen. Diurnal enhancements or pulsations of carbohydrate from photosynthesis may assist the movement of sugar through the sieve tubes.

Experimental water soluble carbohydrate data WSC were given by Dunphy and Hanway (23) for Hark and Amsoy cultivars and by Brevedan *et al.* (8). The results are similar to the simulated values obtained using SOYMOD/OARDC.

Simulated leaf blade TAC concentrations tended to increase from 7.5% at emergence to 13.0% at physiological maturity during 1974. Simulated stem-petiole TAC concentrations increased from about 6% at 20 days after emergence to 14.0% at 90 days and sharply declined thereafter. Prior to 20 days, phloem transport activity was limited.

The high concentration simulated in the leaf blades at physiological maturity is due to the contribu-

tion of starch remaining in the leaves. Various types of carbohydrates, not available for growth but present in the leaves, may be left in the leaves at abscission. The values of the rate parameters for the leaf starch term will govern the amount of reserves left, and may have some impact on final simulated seed yield.

Figures 23a and 23b show simulated nitrogen concentrations for the leaf blades, fruit, and stem-petioles over the growing season. The ranges of simulated values and the predicted behavior are similar to those of Hanway and Weber (33) or Pal and Saxena (66). The young tissue at emergence began with the preset initial value of 6.8%. However, these values declined rapidly to about 4.0% around 20 to 30 days after emergence. Both field and simulated data showed a slight rise in N concentration around flowering for the leaf blades. At this time carbohydrate had reached the nodules and the plant system had begun to generate its own leaf nitrogen supplies. At anthesis, both simulated leaf blade and stem-petiole nitrogen concentrations leveled off and eventually began a slow decline toward physiological maturity. At anthesis, simulated fruit nitrogen began to increase to about 6.8% as the reproductive system became active and remained constant to physiological maturity.

SOYMOD/OARDC represents one of the first attempts to simulate growth in a continuous manner in a crop simulator without the use of an arbitrary carbohydrate switching mechanism. For example, SIMED, a crop simulator for alfalfa developed at Purdue University, assumes a carbohydrate growth switching function which begins to shut off growth at below 8% TAC (41). In SOYMOD/OARDC, soybean growth can occur at any level of carbohydrate from near 0% to more than 50%. However, carbohydrate concentration is stabilized around 8 or 9% because of the partitioning and starch buffering mechanisms. No carbohydrate-growth switch is used in SOYMOD and stabilization occurs because of the closed-loop system of differential equations.

In the case of nitrogen, growth is assumed linearly proportional within given limits as indicated earlier. No growth is assumed to occur below the lower limit (biologically this is probably true), but saturation occurs above the upper limit (see Figure 13). However, simulated N concentrations did not approach the upper limit. There was never enough carbohydrate to achieve this in the presence of fruiting, or during any other stage of growth. Thus, fruit development and N assimilation appear to compete for carbohydrate in the simulator, and this has been shown experimentally to be the case during actual development of the plant in the field.

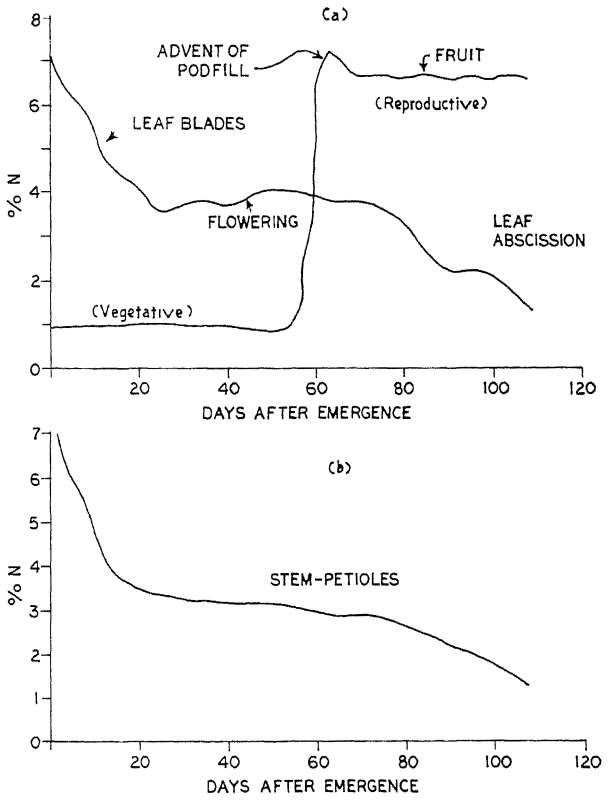

FIGS. 23a and 23b.—Simulated plant nitrogen concentrations (percent N) for successive stages of growth for 1974, (a) for fruit and leaf blades and (b) for stem-petioles.

Seven-Year Summary of Simulated Results

As a further test of SOYMOD, Table 4 shows the simulated yield response for 7 years of recorded weather data from 1971 to 1977. These simulated data assume a crop of disease, weed, and insect-free soybeans.

Each simulation was begun with an emergence date of May 25 and was run to a simulated maturity date. This maturity date is determined in the model when both the final fruit number per plant is resolved and when the fruit dry matter reaches a maximum. The insolation data recorded during the summers of 1975 and 1976 were determined to be in error from separate solar energy studies conducted at OARDC. These were corrected as noted.

Simulated seed yields and plant dry matter varied from year to year. It is best to consider separately what happened vegetatively and reproductively. A suitable date of demarcation of vegetative growth from reproductive growth is the date of the beginning of podfill. For Beeson variety, this usually occurs near the end of July or the first week of August.

TABLE 4.—Comparison of Simulated Yields for Beeson Soybeans Over Several Growing Seasons, Wooster, Ohio.*

Year	Total Season Rainfall Insolation (Podfill-Maturity)		Total PHYSD	Total ET	Simulated Results (per Plant Basis)					
					Date Flower	Date Podfill	Date Maturity	Max Leaf Area	Total DM	Fruit No	Seed Yield
	cm	ly	days	cm	(Days after Emergence)			cm^2	gm		kg/ha
1971	18.5 (2.8)	52,423 (19,903)	120.6	30.5	7/5 (42)	7/26 (63)	9/7 (106)	1581	45.9	37	2836
1972	41.2 (14.2)	46,925 (16,826)	114.7	31.2	7/14 (51)	8/3 (71)	9/13 (112)	1675	45.7	27	3045
1973	32.8 (9.7)	45,477 (15,679)	123.3	32.5	7/4 (41)	7/25 (62)	8/31 (88)	1713	52.6	59	3446
1974	29.2 (16.5)	49,009 (16,564)	113.2	36.6	7/10 (47)	7/30 (67)	9/9 (108)	1760	47.0	35	2791
1975	31.5 (14.7)	43,792† (16,395)	124.4	31.2	7/4 (41)	7/25 (62)	9/1 (100)	1444	31.1	40	1865
1976	31.8 (13.2)	44,499‡ (16,492)	112.4	31.2	7/8 (45)	7/28 (65)	9/8 (107)	1657	44.8	40	2865
1977	47.5 (17.5)	48,546 (14,790)	119.2	34.0	7/7 (44)	7/28 (65)	9/2 (101)	1648	59.2	55	3408
ave.								1639	46.6	42	2894

*Simulated using SOYMOD/OARDC on IBM 370/158, with 76.2 cm row spacing, 5.1 cm plant spacing at emergence, no irrigation water applied, emergence date was May 25, run to the indicated simulated date of maturity.

†1975 insolation data corrected by factor of 1.26.

‡1976 insolation data corrected by factor of 1.1.

The total amount of plant leaf area and total plant dry matter are good measures of vegetative growth. Leaf area reaches a maximum level during the middle of August. Maximum plant dry matter occurs about 1 week later. Fruit numbers per plant and seed yield (kg ha^{-1}) are measures of reproductive growth. The relationships among these values are related to several key meterological data such as rainfall, solar radiation, and temperature, and to the timing of key reproductive events of flowering and podfill. These values are given in Table 4.

There were several good seed yield years, 1972 (3045 kg ha^{-1}), 1973 (3446 kg ha^{-1}), and 1977 (3408 kg ha^{-1}), vs. a poor seed yield year, 1975 (1865 kg ha^{-1}). Fruit numbers per plant are directly related to the timing of flowering and water availability during the reproductive period. Early flowering (41-44 days after emergence) and high water availability during 1973 and 1977 resulted in high simulated fruit numbers, 59 and 55, respectively. In contrast, late flowering (51 days after emergence) in 1972 resulted in a low number of fruit of 27. Earlier flowering resulted in earlier maturity dates. The length of the podfill period is not constant from year to year and is related to rainfall and insolation during podfill.

The seed yield is partially related to the amount of leaf area attained by podfill. A large amount of leaf area often resulted in higher yields. The year 1972 was a high seed yielding year with 3045 kg ha^{-1} (1675 cm^2 leaf area), as was 1973 with 3446 kg ha^{-1} (1713 cm^2 leaf area). Most years with the exception of 1971 had adequate rainfall during reproductive growth. Only 2.8 cm (1.1 inches) occurred during August 1971 compared with an average rainfall of 13.9 cm (5.5 inches). The year 1971 could have been a higher yielding year without this limitation.

The year 1975 was simulated as a low seed yield year (1865 kg ha^{-1}). The total season insolation rate was low (43,792 ly). Even with the solar correction, leaf area (1444 cm) was low and this appears to be the chief cause for the low yield, even though rainfall (14.7 cm) and insolation (16,395 ly) appeared adequate during the month of August.

Based on these results, it appears that SOYMOD/OARDC can be used for year-to-year forecasting. Undoubtedly questions will be asked about the accuracy of these predictions. It must be remembered that the simulated results are merely predictions and some ground-truth data are always helpful.

Of the variables mentioned, only water availability is controllable in the field. The amount of water available during flowering and podfill is important in developing seed yield. The timing of flowering is also an important variable in determining fruit numbers, but is one of the most difficult variables to verify. Plant capacity to support reproductive load must be first attained vegetatively. Rainfall, temperature, and insolation levels must be all favorable during the podfill period (month of August) to attain high level of seed yield.

It is believed that the soybean plant has a remarkable ability to adapt to various conditions. SOYMOD/OARDC is an attempt to mimic some of that adaptability. The use of the model does not preclude the testing of varieties in the field. It can be useful in sorting and summarizing the various observed aspects of crop response for any given growing season. It is, therefore, a tool of research and extension (15, 18).

FUTURE NEEDS

The experimental field data used to validate the simulation model thus far have shown definite limitations in terms of sample size, accuracy, and background cultural and management information. The following recommendations are given in order to improve the quality of future data obtained for validation or verification purposes.

(a) For calibration purposes, a dry matter-time history should include the dry weights of all important morphological parts: leaf blades, stem-petioles, seed and pods, and roots. It would be preferable that these data include dry matter by canopy sections of not more than five nodes each. Leaf areas must also be recorded to validate energy collection surfaces in the model. Fruit numbers and final seed yields must also be recorded with no losses. Timing of node formation should be recorded.

(b) A complete record of all cultural practices, such as application of herbicides, irrigation schedule, cultivation, row and plant spacing, etc.

(c) Planting date, emergence date, and date of final harvest.

(d) Record of significant morphological events: advent and termination of flowering, advent of podfill and physiological maturity, and advent and termination of grand senescence.

(e) Record of insect, disease, and weed problems, and occurrence of severe weather events.

(f) Dry matter sample size must be sufficiently large to obtain good mean and variance estimates.

(g) Record of initial soil moisture and soil moistures throughout the growing season should be obtained to insure the validity of the soil moisture submodel.

(h) Record of soil fertility, type of soil, bulk density, and water holding capacity. Estimate of structural stability (infiltration factor).

It has been found that the use of the Cooper's insolation equation (13), the sinusoidal instantaneous temperature generator using maximum and minimum air temperatures, and the dewpoint assumption (using minimum air temperature where dewpoint is not available) is probably adequate for simulation studies involving the current quality of field data. Dewpoint temperatures should be recorded if possible. However, greater resolution of weather data (*e.g.*, weather records every half-hour or hour) may be required for higher calibration precision.

This bulletin describes an advanced plant simulation system. A considerable amount of detailed output is possible using this simulator, much more than can be probably validated with the field data currently available. It is very difficult to conceive of a simpler system that would generate this level of detailed information.

Improvements in the simulator could involve the following areas of research:

a) A detailed restructuring of the root system and soil moisture balance. A considerable amount of good literature is available to support this.

b) A detailed description of the xylem system and mechanism of nitrogen partitioning needs to be defined.

c) The introduction of management and cultural practices.

d) Improvement is needed in the timing of flowering and podfill. The present phenological equation appears too sensitive to temperature, and may not be valid for other climatological locations.

e) Validation of SOYMOD/OARDC at other locations where soybean crop production is important.

SUMMARY

SOYMOD/OARDC is a detailed computer simulator of the soybean plant. It attempts to provide process description and visual description of the plant. An important key in this system is the breakdown and description of dry matter as the sum of four major entities: structural carbohydrate, available carbohydrate, starch, and protein. The mass balance system which encompasses the soil and aerial environment assumes that no mass is created or destroyed, but is transferred to or from the environment by the plant system. Material within the plant is partitioned among the morphological parts: leaf blades, stem-petioles, fruit, and roots. Available carbohydrate is transported in the plant, and the mechanism for this has been described using a system of coupled partial differential equations. The rates of material loss from one entity subsystem must be balanced by the rate of gain in another entity subsystem or returned to the environment.

Simulation of soybeans or plants in general requires an adequate description of the internal control system. This feature of the plant living system has eluded the crop modeling community for some time. A modest but satisfactory amount of dynamic control is provided by a plant carbon-nitrogen balance. By expressing the role of carbon in the nitrogen balance and concurrently, the role of nitrogen in the carbon balance, the two systems are linked and work together as a function of rate parameters and environmental conditions.

Carbon-nitrogen or dry matter-nitrogen ratios have little meaning to the total system unless they can be related to a general purpose of the system or specific subsystems. This purpose is assumed to be mass transport and mass conversion within the plant system, in response to specific cues to resolve internal deficiencies at given locations.

A complete internal control network has not been formulated. Before the internal control network can be expanded, some agreement must be reached on what additional components should be modeled or related to the rest of the system. The system should encompass all of the components possible.

SOYMOD/OARDC is an attempt to describe the soybean plant on the basis of carbon and nitrogen. This living system obviously depends on other nutrient components as well: phosphorous, potassium, and iron, for example. Future simulation efforts will address these.

The spectrum of simulated results from this model means that simpler soybean models can be questioned. Statistically based crop models with claims of accuracy and great utility should be judged in perspective. Inferential statistics were developed to aid in the testing of theories, but were never intended to designate what the theory should be.

The soybean model described in this manuscript is the original OARDC version to which reference should be made. Since May 1978, versions of SOYMOD/OARDC have been run on computers located at Wooster, Ohio, and Lincoln, Nebraska, under separate research programs. Over the past year, addi-

tional tests and simulation runs have been performed on SOYMOD/OARDC. Not all of the results of these simulations are described here, but will be presented in future publications.

Copies of the model will be made available to state or federal agricultural researchers provided full credit is made public. However, the authors assume no liability for results generated on machines outside their domain. SOYMOD/OARDC and more recent versions are not available as an extension tool, since this simulator is most suitable for research and teaching involving physiological processes of the soybean.

REFERENCES

1. Abernathy, R. H., R. G. Palmer, R. Shibles, and I. C. Anderson. 1977. Histological Observations on Abscissing and Retained Soybean Flowers. Can. J. Plant Sci., 57:713-716.
2. Arya, L. M., D. A. Farrel, and G. R. Blake. 1975. A Field Study of Soil Water Depletion Patterns in Presence of Growing Roots: III. Rooting Characteristics and Root Extraction of Soil Water. Proc., Soil Sci. Soc. Am., 39(3): 437-444.
3. Baker, C. H. and R. Bruce Curry. 1976. Structure of Agricultural Simulators: A Philosophical View. Agricultural Systems (Great Britain), 1:201-218.
4. Baker, C. H., R. B. Curry, and J. G. Streeter. SOYMOD II. Unpublished version.
5. Beuerlein, J. E. and J. W. Pendleton. 1971. Photosynthetic Rates and Light Saturation Curves of Individual Soybean Leaves Under Field Conditions. Crop Sci., 11:217-219.
6. Blad, B. L. and D. G. Baker. 1972. Orientation and Distribution of Leaves Within Soybean Canopies. Agron. J., 64:26-29.
7. Brady, R. A., F. M. Goltz, W. L. Powers, and E. T. Kanemasu. 1977. Relation of Soil Water Potential to Stomatal Resistance of Soybeans. Agron. J., 69:97-99.
8. Brevedan, R. E., D. B. Egli, and J. E. Leggett. 1977. Influence of N Nutrient on Total N, Nitrate, and Carbohydrate Levels in Soybeans. Agron. J., 69:965-969.
9. Buttery, B. R. and R. I. Buzzell. 1977. The Relationship Between Chlorophyll Content and Rate of Photosynthesis in Soybeans. Can. J. Plant Sci., 57(1):1-5.
10. Chailakhyan, M. K. 1968. Internal Factors of Plant Flowering. Ann. Rev. Plant Physiol., 19:1-36.
11. Childs, S. W., J. R. Gilley, and W. E. Splinter. 1977. A Simplified Model of Corn Growth Under Moisture Stress. Trans., ASAE, 20(5): 858-865.
12. Christy, A. L. and J. M. Ferrier. 1973. A Mathematical Treatment of Munch's Pressure-Flow Hypothesis of Phloem Translocation. Plant Physiol., 52:531-538.
13. Cooper, P. I. 1969. Digital Simulation of Transient Solar Processes. Solar Energy, 12: 313-331.
14. Curry, R. B. and L. H. Chen. 1971. Dynamic Simulation of Plant Growth—Part II. Incorporation of Actual Daily Weather and Partitioning of New Photosynthate. Trans., ASAE, 14(6): 1170-1174.
15. Curry, R. B. and J. G. Streeter. 1977. A New Approach Developed for Understanding Soybeans. OARDC, Ohio Report, 62(3):44-47.
16. Curry, R. Bruce, C. H. Baker, and J. G. Streeter. 1975. An Overview of Soymod, Simulator of Soybean Growth and Development. Proc., 1975 Summer Computer Simulation Conferences, July 21-23, 1975, San Francisco, pp. 954-960.
17. Curry, R. B., C. H. Baker, and J. G. Streeter. 1975. SOYMOD I: A Dynamic Simulator of Soybean Growth and Development. Trans., ASAE, 18(5) 963-974.
18. Curry, R. B., G. E. Meyer, J. G. Streeter, and H. J. Mederski. 1980. Simulation of the Vegetative and Reproductive Growth of Soybeans. World Soybean Research Conference II, Proc., pp. 557-570. Westview Press, Boulder, Colo.
19. deWit, C. T. 1960. On Competition. Versl. Landbouwk. Onderz., 66(8), 82 pp.
20. deWit, C. T. 1965. Photosynthesis of Leaf Canopies. Agri. Res. Report No. 663, Center for Agricultural Publications and Documentation, Wageningen, The Netherlands, 57 pp.
21. Dornhoff, G. M. and R. M. Shibles. 1970. Varietal Differences in New Photosynthesis of Soybean Leaves. Crop Sci., 10:42-45.
22. Duncan, W. G., R. S. Loomis, W. A. Williams, and R. Hanau. 1967. A Model for Simulating Photosynthesis in Plant Communities. Hilgardia, 28:181-205.
23. Dunphy, E. J. and J. J. Hanway. 1976. Water-Soluble Carbohydrate Accumulation in Soybean Plants. Agron. J., 68(5):697-700.
24. Dure, L. S. 1975. Seed Formation. Annu. Rev. Plant Physiol., 26:259-278.
25. Egli, D. B. 1975. Rate of Accumulation of Dry

Weight in Seed of Soybeans and Its Relationship to Yield. Can. J. Plant Sci., 55:215-219.

26. Fehr, W. R., C. E. Caviness, D. T. Burmood, and J. S. Pennington. 1971. State of Development Descriptions for Soybeans, *Glycine max.* (L.) Merrill. Crop Sci., 11:929-931.
27. Ferrier, J. M. and A. L. Christy. 1975. Time-dependent Behavior of a Mathematical Model for Munch Translocation. Plant Physiol., 55: 511-514.
28. Fisher, D. B. 1975. Structure of Functional Soybean Sieve Elements. Plant Physiol., 56: 555-569.
29. Fisher, J. E. 1963. The Effects of Short Days on Fruitset as Distinct from Flower Formation in Soybeans. Can. J. Botany, 41:971-973.
30. Forrester, J. W. 1961. Industrial Dynamics. MIT Press, Boston.
31. Hamner, K. C. 1969. *Glycine max.* (L.) Merrill. *In* Evans, L. T., The Induction of Flowering, Some Case Histories. Cornell Univ. Press, Ithaca, N. Y.
32. Hanson, W. D., R. C. Leffel, and R. W. Howell. 1963. Genetic Analysis of Energy Production in the Soybean. Crop Sci., 1:121-126.
33. Hanway, J. J. and C. R. Weber. 1971. Accumulation of N, P, and K by Soybean *(Glycine max.* (L.) Merrill) Plants. Agron. J., 63:406-408.
34. Hanway, J. J. and C. R. Weber. 1971. Dry Matter Accumulation in Eight Soybean *(Glycine max.* (L.) Merrill) Varieties. Agron. J., 63: 227-230.
35. Hanway, J. J. and C. R. Weber. 1971. Dry Matter Accumulation in Soybean *(Glycine max.* (L.) Merrill) Plants as Influenced by N, P, and K Fertilization. Agron. J., 63:263-266.
36. Hesketh, J. D. and J. W. Jones. 1976. Some Comments on Computer Simulators for Plant Growth—1975. Ecological Modeling, 2:235-247.
37. Hesketh, J. D., D. L. Myhre, and D. R. Willey. 1973. Temperature Control of Time Intervals Between Vegetative and Reproductive Events in Soybeans. Crop Sci., 13:250-254.
38. Hicks, D. R. and J. W. Pendleton. 1969. Effect of Floral Bud Removal on Performance of Soybeans. Crop Sci., 9:435-437.
39. Hill, R. W., D. R. Johnson, and K. U. Ryan. 1979. A Model for Predicting Soybean Yields from Climatic Data. Agron. J., 71:251-256.
40. Hofstra, G., J. D. Hesketh, and D. L. Myhre. 1977. A Plastochron Model for Soybean Leaf and Stem Growth. Can. J. Plant Sci., 57:167-175.
41. Holt, D. A., R. J. Bula, G. E. Miles, M. M. Schreiber, and R. M. Peart. 1975. Environmental Physiology, Modeling and Simulation of Alfalfa Growth. I. Conceptual Development of SIMED. Purdue Univ., AES Bull. 907, 26 pp.
42. Housley, T. L. and D. B. Fisher. 1977. Estimation of Osmotic Gradients in Soybean Sieve Tubes by Quantitative Autoradiography. Plant Physiol., 59:701-706.
43. Howell, R. W. 1950. Physiology of the Soybean. USDA Pub. No. 338, U. S. Regional Soybean Laboratory, Urbana, Ill.
44. Hunt, W. F. and R. S. Loomis. 1976. Carbohydrate-Limited Growth Kinetics of Tobacco *(Nicotiana rustica* L.) Callus. Plant Physiol., 57:802-805.
45. Ishizuka, Y. 1969. Engineering for Higher Yields. *In* Physiological Aspects of Crop Yields, edited by J. D. Eastin, *et al.,* Amer. Soc. Agri. Eng., Madison, Wis., 396 pp.
46. Jones, J. W., J. D. Hesketh, E. J. Kamprath, and H. D. Bowen. 1974. Development of Nitrogen Balance for Cotton Growth Models: A First Approximation. Crop Sci., 14:541-546.
47. Keener, H. M. and G. E. Meyer. 1978. Transient Solutions of Differential Equations on the Digital Computer by Approximation and Solution as First Order Equations. In review for publication.
48. Lang, A. 1978. A Model of Mass Flow in the Phloem. Aust. J. Plant Physiol., 5:535-546.
49. Lang, A. 1978. Interactions Between Source, Path, and Sink in Determining Phloem Translocation Rate. Aust. J. Plant Physiol., 5:665-674.
50. Leopold, A. C. 1959. Experimental Modification of Plant Senescence. Plant Physiol., 34: 570-573.
51. Lindoo, S. J. and L. D. Nooden. 1977. Studies on the Behavior of the Senescence Signal in Anoka Soybeans. Plant Physiol., 59:1136-1140.
52. Lindoo, S. J. and L. D. Nooden. 1976. The Interrelation of Fruit Development and Leaf Senescence in 'Anoka' Soybeans. Bot. Gaz., 137(3):218-223.
53. Lockhart, J. A. 1976. Plant Growth, Assimilation, and Development: A Conceptual Framework. Bio Science, 26(5):332-338.
54. Lommen, P. W., C. R. Schwintzer, C. S. Yocum, and D. M. Gates. 1971. A Model Describing Photosynthesis in Terms of Gas Diffusion and Enzyme Kinetics. Planta, 98:195-220.

55. Maas, Stephen J. and Gerald F. Arkin. 1978. User's Guide to SORGF: A Dynamic Grain Sorghum Growth Model with Feedback Capacity. Program and Model Documentation No. 78-1, Texas Agri. Exp. Sta., College Station.

56. Mahler, H. R. and E. H. Cordes. 1968. Basic Biological Chemistry. Harper & Row, Publishers, New York, 527 pp.

57. Major, D. J., D. R. Johnson, J. W. Tanner, and I. C. Anderson. 1975. Effects of Daylength and Temperature on Soybean Development. Crop Sci., 15:174-179.

58. Meyer, B. S., D. B. Anderson, and R. M. Bohning. 1963. Introduction to Plant Physiology. D. Van Nostrand Co., Inc., Princeton, N. J., p. 327.

59. Meyer, G. E., R. B. Curry, J. G. Streeter, and C. H. Baker. 1978. Analysis and Computer Simulation of Flowering and Reproductive Growth in Indeterminant Soybeans. Paper No. 78-4025, Annual Meeting, Amer. Soc. Agri. Eng., Logan, Utah.

60. Monteith, J. L. 1965. Light Distribution and Photosynthesis in Field Crops. Ann. Bot., London (N. S.), 29:17-37.

60a. Monteith, J. L. 1965. Evaporation and Environment. Symposium, Soc. Exp. Biol., 19: 205-234.

61. Munch. 1930. Die Stouffbewegungen in der Pflanze. Jeana: Gustav Fischer.

62. Murata, Y. 1975. The Effect of Solar Radiation, Temperature, and Aging on Net Assimilation Rate of Crop Stands, from the Analysis of the Maximal Growth Rate Experiment of IBP/PP. II. The Case of Maize and Soybean Plants. Proc., Crop Sci. Soc. Japan, 44(2):160-165.

63. Nafziger, E. D. and H. R. Koller. 1976. Influence of Leaf Starch Concentration on CO_2 Assimilation in Soybeans. Plant Physiol., 57: 560-563.

64. Nobel, Park S. 1974. Introduction to Biophysical Plant Physiology. Univ. Calif., Los Angeles, W. H. Freeman and Co., San Francisco, 488 pp.

65. Ojima, M., J. Fukui, and Iwoo Watanabe. 1965. Studies on the Seed Production of Soybean. II. Effect of Three Major Nutrient Elements, Supply, and Leaf Age on the Photosynthetic Activity and Diurnal Changes in Photosynthesis of Soybean Under Constant Temperature and Light Intensity. Crop Sci. Soc. Japan, 33:437-442.

66. Pal, U. R. and M. C. Saxena. 1976. Relationship Between Nitrogen Analysis of Soybean Tissues and Soybean Yields. Agron. J., 68:927-932.

67. Penning de Vries, F.W.T. 1975. The Cost of Maintenance Processes in Plant Cells. Ann. Bot., 39:77-92.

68. Sakamoto, C. M. and R. H. Shaw. 1967. Light Distribution in Field Soybean Canopies. Agron. J., 59:7-9.

69. Sato, K. 1976. The Growth Responses of Soybean Plant to Photoperiod and Temperature. I. Responses in Vegetative Growth. Proc., Crop Sci. Soc. Japan, 45(3):443-449.

70. Scully, N. J., M. W. Parker, and H. A. Borthwick. 1945. Relationship of Photoperiod and Nitrogen Nutrition to Initiation of Flower Primordia in Soybean Varieties. Bot. Gazette, 107:218-231.

71. Sinclair, T. R. and C. T. deWit. 1976. Analysis of the Carbon and Nitrogen Limitations to Soybean Yield. Agron. J., 68:319-324.

72. Sinclair, T. R. and C. T. deWit. 1975. Photosynthate and Nitrogen Requirements for Seed Production by Various Crops. Science, 565-567.

73. Splinter, W. E. 1974. Modeling of Plant Growth for Yield Prediction. Agri. Meteorol., 14:243-253.

74. Stapleton, H. N. and R. P. Meyers. 1971. Modeling Subsystems for Cotton—The Cotton Plant Simulation. Trans., ASAE, 14:950-953.

75. Stephenson, R. A. and G. L. Wilson. 1977. Patterns of Assimilate Distribution in Soybeans at Maturity. I. The Influence of Reproductive Development Stage and Leaf Position. Aust. J. Agri. Res., 28:203-209.

76. Streeter, J. G. 1974. Growth of Two Soybean Shoots on a Single Root: Effect on Nitrogen and Dry Matter Accumulation by Shoots and on the Rate of Nitrogen Fixation by Nodulated Roots. J. Expl. Bot., 25:189-198.

77. Sun, C. N. 1957. Histogenesis of the Leaf and Structure of the Shoot Apex in *Glycine max.* (L.) Merrill. Bull., Torrey Botanical Club, 84 (3):163-174.

78. Tayo, T. O. 1977. Effect of Flower or Pod Removal on the Performance of Soya Beans (*Glycine max.* (L.)). J. Agri. Sci., Camb., 89:229-234.

79. Thibodeau, P. S. and E. G. Jaworski. 1975. Patterns of Nitrogen Utilization in the Soybean. Planta, 127:133-147.

80. Thorne, J. E. and H. R. Koller. 1974. Influence of Assimilate Demand on Photosynthesis, Diffusive Resistances, Translocation, and Carbohydrate Levels of Soybean Leaves. Plant Physiol., 54:201-207.
81. Thornley, J. H. M. 1972. A Model of Biochemical Switch, and Its Application to Flower Initiation. Ann. Bot., 36:861-871.
82. Thornley, J. H. M. 1972. A Model to Describe the Partitioning of Photosynthate During Vegetative Plant Growth. Ann. Bot., 36:419-430.
83. Thornley, J. H. M. 1976. Mathematical Models in Plant Physiology. Experimental Botany, An International Series of Monographs, Vol. 8., Academic Press, London, 318 pp.
84. Van Doren, D. 1978. Unpublished Soil Water Retention Data.
85. Waggoner, P. E. 1969. Predicting the Effect Upon New Photosynthesis of Changes in Leaf Metabolism and Physics. Crop Sci., 9:315-321.
86. Warrington, I. J., M. Peet, D. T. Patterson, J. Bruce, R. M. Haslemore, and H. Hellmers. 1977. Growth and Physiological Responses of Soybean Under Various Thermoperiods. Aust. J. Plant Physiol., 4:371-380.
87. Wiersma, J. V. and T. B. Bailey. 1975. Estimation of Leaflet, Trifoliolate, and Total Leaf Areas of Soybeans. Agron. J., 67:26-30.
88. Woodward, R. G. 1976. Photosynthesis and Expansion of Leaves of Soybean Grown in Two Environments. Photosynthetica, 10(3):274-279.
89. Woodward, R. G. and H. M. Rawson. 1976. Photosynthesis and Transpiration in Dicotyledonous Plants. II. Expanding the Senescing Leaves of Soybean. Aust. J. Plant Physiol., 3:257-267.

APPENDIX A:

Summary of Mass Balance Equations

Sets of mass balance equations are written for each node on the shoot and for the root system.

For the leaves at node i, the equations are:

Soluble Sugars $C_L(i)$

$$\frac{1}{G_L(i)} \cdot \frac{\partial C_L(i)}{\partial t} = P_s(i) \cdot A(i) - U_L(i) - Q_L(i) - L(i) \quad (A1)$$

where:

$P_s(i)$ = f(CO_2, K_{ps}, r_s, r_m, P_c, R, i)

$A(i)$ = leaf area at node i

$$U_L(i) = \frac{K_L \cdot \phi_L(N)\ C_L(i)}{K_{ML} \cdot G_L(i) + C_L(i)}$$

$$Q_L(i) = \frac{G_L(i) \cdot K_{SC} \cdot S_L(i) - K_{CS} \cdot C_L^2(i)}{G_L^2(i)}$$

$$L(i) = K_{LP} \cdot \left\{\frac{C_L(i)}{G_L(i)}\right\}^2$$

Reserve Carbohydrates $S_L(i)$

$$\frac{1}{G_L(i)} \cdot \frac{\partial S_L(i)}{\partial t} = \frac{G_L(i) \cdot K_{SC} \cdot S_L(i) - K_{CS} \cdot C_L^2(i)}{G_L^2(i)} \quad (A2)$$

Structural Carbohydrates $G_L(i)$

$$\frac{1}{G_L(i)} \cdot \frac{\partial G_L(i)}{\partial t} = \frac{E_{GL} K_L \cdot \phi_L(N) \cdot C_L(i)}{K_{ML} \cdot G_L(i) + C_L(i)} \quad (A3)$$

Nitrogen Compounds N_L (for all leaves)

$$\frac{1}{G^t_L} \frac{\partial N_L}{\partial t} = \propto_L \left\{\frac{C_R}{G_R}\right\} - \frac{\propto_{FM} N_L}{G^t_L} \quad (A4)$$

where: $G^t_L = \sum_{i=1}^{n} G_L(i)$

Total Leaf Dry Matter DM_L

$$DM_L = G^t_L + C^t_L + S^t_L + N_L \quad (A5)$$

where:

$$C^t_L = \sum_{i=1}^{n} C_L(i)$$

$$S^t_L = \sum_{i=1}^{n} S_L(i)$$

For stem section below node i, the equations are:

Structural Carbohydrate $G_S(i)$

$$\frac{1}{G_S(i)} \cdot \frac{\partial G_S(i)}{\partial t} = \frac{E_{GS}\ K_S\ \phi_S(N)\ C_P(i)}{K_{MS} \cdot G_S(i) + C_P(i)} \quad (A6)$$

Nitrogen Compounds N_S (for all stem parts)

$$\frac{1}{G^t_s} \cdot \frac{\partial N_S}{\partial t} = \propto_S \left\{\frac{C_R}{G_R}\right\} - \propto_{FM} \left\{\frac{N_S}{G_S}\right\} \quad (A7)$$

where: $G_S^t = \sum_{i=1}^{n} G_S(i)$

Total Stem Dry Matter DM_S

$$DM_S = G_S^t + C_P^t + N_S \qquad \text{(A8)}$$

where: $C_P^t = \sum_{i=1}^{n} C_P(i)$

For the phloem, which supplies the stem, fruit, and root system:

Soluble Sugars Only $C_P(i)$

$$\frac{1}{G_S(i)} \cdot \frac{\partial C_P(i)}{\partial t} = K_{LP} \left\{\frac{C_L(i)}{G_L(i)}\right\}^2 - U_F(i) - U_S(i) - \frac{\beta \cdot n(i) \cdot T\, A^2_S}{8\eta\, \pi\, G^2_S(i)} \cdot \frac{C_P(i)\ \{C_P(i+1) - C_P(i)\}}{\Delta y(i)} \qquad \text{(A9)}$$

where: $U_S(i) = \dfrac{K_S\ \phi_S(N)\ C_P(i)}{K_{MS} \cdot G_S(i) + C_P(i)}$

$$U_F(i) = \frac{K_F\ \phi_F(N)\ C_P(i)}{K_{MF} \cdot G_F(i) + C_P\ (i)}$$

For the root system, the transport rate leaving the first internodal section is the rate entering the root:

Thus for Soluble Sugars C_R

$$\frac{1}{G_R}\frac{\partial C_R}{\partial t} = \frac{\beta \cdot n(i) \cdot T\, A_S^2}{\beta\eta\ \pi\ G_S^2(i)} \cdot \frac{C_P(1)\ \{C_P(2) - C_P(1)\}}{\Delta y(1)} - U_R - K_{NS}\left\{\frac{C_R}{G_R}\right\} - G_R \cdot \left\{\frac{K_{SC}\ S_R - K_{CS}\ C_R}{G_R^2}\right\} \qquad \text{(A10)}$$

where: $K_{NS} = \alpha_L + \alpha_S + \alpha_F + \alpha_R$

and $\alpha_L = 1 - \phi_L(N)$
$\alpha_S = 1 - \phi_S(N)$
$\alpha_F = 1 - \phi_F(N)$
$\alpha_R = 1 - \phi_R(N)$

Root Starch S_R

$$\frac{1}{G_R} \cdot \frac{\partial S_R}{\partial t} = \frac{K_{SC}\ S_R - K_{CS}\ C_R}{G_R} \qquad \text{(A11)}$$

Root Structural Carbohydrate G_R

$$\frac{1}{G_R}\frac{\partial G_R}{\partial t} = \frac{E_{GR}\ K_R\ \phi_R(N)\ C_R}{K_{MR}\ G_R + C_R} \qquad \text{(A12)}$$

Root Nitrogen Compounds

$$\frac{1}{G_R}\frac{\partial N_R}{\partial t} = \alpha_R \left\{\frac{C_R}{G_R}\right\} \qquad \text{(A13)}$$

Note that nitrogen partitioning priorities are set by the ϕ functions which express the role of N in carbohydrate utilization.

APPENDIX B:
Description of SOYMOD/OARDC Program Units

Program Routine	Size (bytes)	Description and Purpose
ALEAF	246	Linearized carbohydrate mass balance equation for leaves at any node, net assimilate rate from subroutine PHOTO, growth, starch, and export to the phloem.
COLEF	66	Leaf area conversion factor (cm^2 per gram) based on estimated leaf age.
DRPLF	740	Checks conditions for a specific or general leaf fall as a result of senescence.
FLWR2	1272	Describes flowering and podfill events as a function of average temperature and day length using equations by Major, et al. (57).
GNSIS	246	Linearized carbohydrate mass balance equation for apical leaf: photosynthesis, growth, and partial export to leaf primordia.
GRWTH	260	Generalized routine for computing growth rate based on a linearized Michaelis-Menten equation, "enzyme" effect is given by PNCT2.
MAINLINE	32,024	Schedules and cues subroutines, sets initial conditions, prompts for required data.
PCHK2	274	Controls rate of photosynthesis based on leaf starch.
PHLOM	566	Carbohydrate mass balance equation for phloem mass transport system.
PHOTO	2144	Computes net photosynthetic rate based on light, CO_2, temperature, nitrogen concentration, and leaf water potential, partially based on Lommen (54).
PHYSS	326	Provides running account of the physiological age of the plant in PHYS days.
PNCT2	532	Determines growth "enzyme" activity based on dry matter-nitrogen status for each plant part.
PRNTR	2574	Prepares and scales weather input (average temperature, daily insolation, day-length, physiological days, soil moisture, planting configuration), and plant dry matter response, leaf area, plant height and number of fruits for output.
ROOT	274	Carbohydrate mass balance equation for the root system, storage, growth, inflow from phloem, and nitrogen fixation.
RPOLE	244	First-order explicit numerical method for high speed integration.
SETUP	1024	Computes diurnal instantaneous air temperatures from max and min temperatures, insolation and Photosynthetically Active Radiation rate from total daily insolation.
SHADE	334	Computes incident light at leaf layer under consideration. Assumes maximum leaf area exposure for any given pair of leaves to incident light (minimum overlap). Odd nodal leaves are only shaded by odd leaves, even nodal leaves are only shaded by even nodal leaves.
FRUIT	466	Computes final fruit number for node considered, based on the rate of advance of reproductive dry matter after 3 days of pod fill. Individual seed growth rate is assumed constant.
SNODE	516	Describes node formation events, computes internodal lengths and total shoot length for given elongation rates.
STORE	1660	Prepares and scales data describing the processes and dry matter components of the plant on a nodal basis. These include partitioned nitrogen, available carbohydrate, starch, and structural carbohydrate weights for each part. It also includes leaf area, fruit numbers, and the magnitude of each term in the mass balance.
WATER	650	Computes evapotranspiration rate based on insolation level, dry bulb and dew-point temperatures, wind velocity. Calculates a soil moisture balance.
STEM	436	Computes current stem diameter and corresponding number of sieve tubes for Munch mass flow system.
DISPLAY	300	Prepares and prints a final summary output for the entire growing season.

APPENDIX C:
SAMPLE OUTPUT

This appendix provides samples of the three types of output produced by SOYMOD/OARDC. In the first example, a chronological log of dry matter accumulation plus physiological, rainfall, and irrigation events are shown starting with initial conditions on day 1 (day of emergence). Information is given in the heading relating to the particular simulation run, the parameters tabulated, and their respective units.

Note that initially weights are in milligrams per meter squared and change to grams per meter squared as the season proceeded. For brevity, the log shown skips segments of the season in order to show output of phenological events as well as occurrence of rainfall, and in this case timing of automatic irrigation. In this example the output days were printed on a 5-day interval, but the program also provides for 1-day or 10-day intervals or for a log of the last day of the season.

The second example shown is the partitioning summary. This output summarizes several parameters by node: 1) rates of net photosynthesis (NET PS), carbohydrate utilization for growth (UTIL), storage (STOR), respiration (RESP), and translocation (OUT) rates in milligrams per hour for each plant part (LEAF, FRUIT, STEM, PHLOM, and (for node 1) ROOTS and XYLEM); 2) dry matter accumulation in the form of protein (PR), total available carbohydrate (TAC) in soluble sugars (SOL), and starch (STAR) and structure (STRUC) in milligrams for each plant part; 3) leaf area at each node in centimeters squared; and 4) number of fruit. For brevity only the first 10 nodes are shown for day 76. The simulator provides for selection of the days for printing the partitioning summary by setting an input parameter at the start of the run.

The third output shown is the short summary. This summary documents many parameters which are given in more detail in the other two output summary reports. The items in this short summary are self-explanatory.

OARDC SOYBEAN GROWTH AND DEVELOPMENT SIMULATOR
HP 3000 SOYMOD LOG

VARIETY BEESON — SUMMER 1974
IRRIGATION IS ON — ROW SPACING(IN) 30.0
PLANT SPACING(IN) 2.0

PRINT CUE 10 HOURS AFTER SUNRISE — PAGE 1

	WEATHER INPUT						PLANT RESPONSE						
TIME DATE	DAYS AFTR EMRG	AVE. DAILY TEMP. C	INSOL. LY	DAY-LGTH. HR	PHYS. TIME DAYS	SOIL MOIST %	MAX. PS MGH/CM2	LEAF WT	STEM WT	ROOT WT	FRUIT WT	LEAF AREA CM2	PL. HT CM	NO FRT
							TOTAL DRY MATTER-MGM-							
05/25	1	10.8	276.	14.8	.2	21.4	.08 134.8	94.6	95.8	1.6	4.5	.0	0	
							TOTAL DRY MATTER- GM-							
06/19	26	18.3	315.	15.1	22.5	17.9	.34 1.0	1.0	.3	.0	198.1	11.7	0	
06/30	37				RAIN .(.02 IN.)									
07/01	38				IRRIG.(.29 IN.)									
07/02	39				IRRIG.(.29 IN.)									
07/03	40				UNIFOLIOLATE DROP(NODE 2)									
07/04	41				IRRIG.(.29 IN.)									
07/04	41	26.4	562.	15.0	38.5	15.0	.30 2.6	2.7	.6	.0	529.7	27.0	0	
07/05	42				IRRIG.(.29 IN.)									
07/05	42				COTYLEDON DROP(NODE 1)									
07/07	44				IRRIG.(.29 IN.)									
07/08	45				IRRIG.(.29 IN.)									
07/09	46				IRRIG.(.29 IN.)									
07/09	46	25.6	515.	14.9	45.0	18.1	.37 3.1	3.5	.7	.0	655.5	35.0	0	
07/10	47				FLOWERS(NODE 4)									
07/29	66	21.7	315.	14.5	68.5	19.5	.37 6.2	7.9	1.3	.0	1344.7	63.6	42	
07/30	67				POD FILL(NODE 4)									
08/01	69				FLOWERS(NODE 11)									
08/01	69				IRRIG.(.29 IN.)									
08/02	70				POD FILL(NODE 5)									
08/02	70				IRRIG.(.29 IN.)									
08/02	70				RAIN .(.75 IN.)									
08/03	71				POD FILL(NODE 6)									
08/03	71				FLOWERS(NODE 12)									
08/28	96	16.9	68.	13.3	104.1	26.7	.13 5.9	8.2	1.8	9.7	1360.3	63.6	55	
08/29	97				POD FILL(NODE 16)									
08/29	97				RAIN .(.85 IN.)									
08/31	99				POD FILL(NODE 17)									
08/31	99				RAIN .(.08 IN.)									
08/31	99				LEAF AND PETIOLE DROP(NODE 6)									
09/08	107	17.5	368.	12.8	112.3	29.6	.00 .0	6.2	2.1	17.5	.0	63.6	31	

SIMULATION RUN COMPLETED

SOYMOD/OARDC
PARTITIONING SUMMARY
SUMMER 1974 LOCATION WOOSTER
PRINT CUE 8 HOURS AFTER SUNRISE PAGE 1

DAY NO.	NODE	PLANT PART	NET PS MGH	CHO UTIL. MGH	PARTITIONING RATES STOR. MGH	RESP. MGH	OUT MGH	PR. MG	TAC SOL. MG	STAR. MG	STRUC MG
76	10	LEAF	.01	.00	.00	.01	.00	89.1	.0	7.0	353.5
		FRUIT	.00000.00		.00	000.00	.00	000.0	.0	.0	1.0
		STEM	.00	.52	.00	5.54	.00	86.7	.0	.0	434.4
		PHLOM	.00	.00	-20.82	.00	14.77	.0	80.4	.0	.0
		-NUMBER OF FRUITS		6-		LEAF AREA		104.5 CM2			
76	9	LEAF	.01	.00	.00	.01	.00	89.1	.0	8.1	376.2
		FRUIT	.00000.00		.00	000.00	.00	000.0	.0	.0	1.0
		STEM	.00	.49	.00	5.59	.00	86.7	.0	.0	447.6
		PHLOM	.00	.00	-22.75	.00	16.67	.0	79.8	.0	.0
		-NUMBER OF FRUITS		6-		LEAF AREA		110.6 CM2			
76	8	LEAF	-.00	.00	-.00	.00	.00	89.1	.0	18.1	447.6
		FRUIT	.00000.00		.00	000.00	.00	000.0	.0	.0	1.0
		STEM	.00	.47	.00	5.63	.00	86.7	.0	.0	456.6
		PHLOM	.00	.00	-25.14	.00	19.05	.0	79.3	.0	.0
		-NUMBER OF FRUITS		6-		LEAF AREA		130.8 CM2			
76	7	LEAF	-.00	.00	-.00	.00	.00	89.1	.0	9.3	402.1
		FRUIT	.00	51.07	.00	1.03	.00	19.1	.0	.0	26.1
		STEM	.00	.42	.00	5.46	.00	86.7	.0	.0	470.3
		PHLOM	.00	.00	-144.06	.00	68.47	.0	72.7	.0	.0
		-NUMBER OF FRUITS		6-		LEAF AREA		116.8 CM2			
76	6	LEAF	-.00	.00	-.00	.00	.00	89.1	.0	9.1	381.3
		FRUIT	.00	11.71	.00	12.02	.00	19.1	.0	.0	450.9
		STEM	.00	.41	.00	5.38	.00	86.7	.0	.0	470.7
		PHLOM	.00	.00	-44.34	.00	14.29	.0	70.7	.0	.0
		-NUMBER OF FRUITS		6-		LEAF AREA		110.2 CM2			
76	5	LEAF	-.00	.00	-.00	.00	.00	89.1	.0	9.1	405.9
		FRUIT	.00	12.03	.00	11.59	.00	19.1	.0	.0	437.4
		STEM	.00	.40	.00	5.32	.00	86.7	.0	.0	473.9
		PHLOM	.00	.00	-37.88	.00	7.58	.0	68.9	.0	.0
		-NUMBER OF FRUITS		3-		LEAF AREA		116.7 CM2			
76	4	LEAF	-.00	.00	-.00	.00	.00	89.1	.0	5.6	328.5
		FRUIT	.00	5.66	.00	16.65	.00	19.1	.0	.0	762.7
		STEM	.00	.40	.00	5.29	.00	86.7	.0	.0	475.9
		PHLOM	.00	.00	-7.04	.00	-14.69	.0	68.0	.0	.0
		-NUMBER OF FRUITS		4-		LEAF AREA		93.9 CM2			
76	3	LEAF	-.00	.00	-.00	.00	.00	89.1	.0	5.5	344.0
		FRUIT	.00000.00		.00	.03	.00	000.0	.0	.0	1.0
		STEM	.00	.38	.00	5.31	.00	86.7	.0	.0	482.2
		PHLOM	.00	.00	20.45	.00	-42.39	.0	67.8	.0	.0
		-NUMBER OF FRUITS		0-		LEAF AREA		97.6 CM2			
76	2	LEAF	000.00	.00	-.00	.00	.00	000.0	.0	000.0	.0
		FRUIT	.00000.00		.00	.03	.00	000.0	.0	.0	1.0
		STEM	.00	.43	.00	5.18	.00	86.7	.0	.0	458.7
		PHLOM	.00	.00	42.56	.00	-63.52	.0	67.7	.0	.0
		-NUMBER OF FRUITS		0-		LEAF AREA		.0 CM2			
76	1	LEAF	000.00	.00	-.00	.00	.00	000.0	.0	000.0	.0
		FRUIT	.00000.00		.00	.03	.00	000.0	.0	.0	1.0
		STEM	.00	.38	.00	5.32	.00	86.8	.0	.0	486.5
		PHLOM	.00	.00	62.47	.00	-84.56	.0	67.6	.0	.0
		ROOTS	.00	3.66	23.34	1.22	.00	321.5	37.1	1.5	1251.9
		XYLEM	69.98	.00	.00	.00	.00	.0	.0	.0	.0
		-NUMBER OF FRUITS		0-		LEAF AREA		.0 CM2			

SIMULATED CROP PERFORMANCE
SOYMOD/OARDC

LOCATION	WOOSTER	SUMMER	1974
VARIETY	BEESON	SOIL TYPE	WSILTL
IRRIGATION	ON	TOTAL IRR.(IN)	10.1
ROW SPACING(IN)	30.0	PLANT SPACING(IN)	2.0

PHYSIOLOGICAL EVENTS

EMERGENCE DATE	05/25	(0 DAE)
FLOWER DATE	07/10	(47 DAE)
PODFILL DATE	07/30	(67 DAE)
MATURITY DATE	09/08	(107 DAE)
GRAND SENESCENCE	09/03	(102 DAE)

WEATHER SUMMARY

TOTAL INSOLATION(LY)	49444.0
HEAT UNITS (PHYS. DAYS)	112.3
TOTAL RAINFALL(IN)	11.5
TOTAL WIND RUN(MI)	6813.0

CROP SUMMARY

PLANT HEIGHT(CM)	63.6	MAX. STEM DIAM(CM)	1.36
MAX LEAF AREA(CM2)	1745.	OCCURRED 84 DAE	
MAX. PLANT DM(GMS)	27.52	OCCURRED 84 DAE	
NUMBER OF NODES	18	TOTAL ET(IN)	16.9
FINAL FRUIT NO.	31	FINAL FRUIT WT.(GMS)	17.5
GRAMS PER 100 SEED	18.8	SEED YIELD(BU/AC)	35.0

*DAE - DAYS AFTER EMERGENCE

BETTER LIVING IS THE PRODUCT

of research at the Ohio Agricultural Research and Development Center. All Ohioans benefit from this product.

Ohio's farm families benefit from the results of agricultural research translated into increased earnings and improved living conditions. So do the families of the thousands of workers employed in the firms making up the state's agribusiness complex.

But the greatest benefits of agricultural research flow to the millions of Ohio consumers. They enjoy the end products of agricultural science—the world's most wholesome and nutritious food, attractive lawns, beautiful ornamental plants, and hundreds of consumer products containing ingredients originating on the farm, in the greenhouse and nursery, or in the forest.

The Ohio Agricultural Experiment Station, as the Center was called for 83 years, was established at The Ohio State University, Columbus, in 1882. Ten years later, the Station was moved to its present location in Wayne County. In 1965, the Ohio General Assembly passed legislation changing the name to Ohio Agricultural Research and Development Center—a name which more accurately reflects the nature and scope of the Center's research program today.

Research at OARDC deals with the improvement of all agricultural production and marketing practices. It is concerned with the development of an agricultural product from germination of a seed or development of an embryo through to the consumer's dinner table. It is directed at improved human nutrition, family and child development, home management, and all other aspects of family life. It is geared to enhancing and preserving the quality of our environment.

Individuals and groups are welcome to visit the OARDC, to enjoy the attractive buildings, grounds, and arboretum, and to observe first hand research aimed at the goal of Better Living for All Ohioans!

The State Is the Campus for Agricultural Research and Development

Ohio's major soil types and climatic conditions are represented at the Research Center's 12 locations.

Research is conducted by 15 departments on more than 7000 acres at Center headquarters in Wooster, eight branches, Pomerene Forest Laboratory, North Appalachian Experimental Watershed, and The Ohio State University.

Center Headquarters, Wooster, Wayne County: 1953 acres

Eastern Ohio Resource Development Center, Caldwell, Noble County: 2053 acres

Jackson Branch, Jackson, Jackson County: 502 acres

Mahoning County Farm, Canfield: 275 acres

Muck Crops Branch, Willard, Huron County: 15 acres

North Appalachian Experimental Watershed, Coshocton, Coshocton County: 1047 acres (Cooperative with Science and Education Administration/Agricultural Research, U. S. Dept. of Agriculture)

Northwestern Branch, Hoytville, Wood County: 247 acres

Pomerene Forest Laboratory, Coshocton County: 227 acres

Southern Branch, Ripley, Brown County: 275 acres

Vegetable Crops Branch, Fremont, Sandusky County: 105 acres

Western Branch, South Charleston, Clark County: 428 acres